UNIVERSIDADE DE LISBOA
FACULDADE DE CIÊNCIAS
DEPARTAMENTO DE QUÍMICA E BIOQUÍMICA

Development of Cellular Models for NIS Functional Expression

Bruno Alexandre Dias Martins

Mestrado em Bioquímica

Especialização em Bioquímica Médica

Dissertação orientada por:
Doutora Ana Luísa Silva
Doutor Federico Herrera

2021

“Nobody is gonna hit as hard as life, but it ain´t how hard you can hit. It’s how hard you can get hit and keep moving forward. It’s how much you can take, and keep moving forward. That’s how winning is done.”

(Rocky Balboa – 2006)

Acknowledgments

This dissertation was only possible due the contribution of several people and institutions that I would like to thank in advanced. This project was made in the Endocrinology Tumors and Signalling Group, in the Department of Endocrinology Diabetes and Metabolism of Hospital de Santa Maria, Centro Hospitalar Universitário de Lisboa Norte (HSM-CHULN) and Ecogenetic and Human Health Lab of the Instituto de Saúde Ambiental (ISAMB). This work would not be possible without the assistance and commitment of the individuals involved.

First I would like to express my greatest gratefulness to Doutora Ana Luísa Silva that gave me the opportunity to do this project with her. Thank you for the shared knowledge and the motivation that you gave me to do it. It was a pleasure to work with you, not only because of the professional you are, but also because of the person you are. I hope we will meet again in the future.

To Doutor Paulo Matos, a special thank you. This project would not be possible without your vision and ideas that helped it to go further.

I would also like to thank to the other members of the Endocrinology Tumors and Signalling Group, Rita Domingues, Patrícia Costa and Márcia Faria that helped me during my project and helped to maintain a very good work environment. Thank you for the ideas, laughs and experiences that you shared. It was a pleasure to know you. This project would not be the same without you.

To Joana Ferreira and Carolina Santos, both Ecogenetic and Human Health Lab. collaborators, my deepest thank you. It was a pleasure to share the lab with you. You are very genuine and good people. I wish you the best.

To Professor Manuel Bicho, Head of the Ecogenetic and Human Health Lab in ISAMB and to Professor Maria João Bugalho, head of the Endocrinology department in HSM-CHULN, thank you for giving me the opportunity to join the ETS research group.

I would also like to thank my friends and family for always believing in me, for helping me to continue my journey and to achieve my goals, for the love and compassion that you gave me through my life. I believe I am the person I am today because of you. Thank you from the bottom of my heart.

Lastly and foremost, a special thank you to my parents, my sister, and my girlfriend for all the support, for all the love, patience and for helping me grow. Thank you for allowing me to follow my dreams, to encourage me to dream higher and for always believing in me. I owe everything to you. I love you.

Abstract

The sodium/iodide symporter (NIS or SLC5A5) is an intrinsic plasma membrane glycoprotein that mediates active transport of iodide into the thyroid follicular cells. NIS mediated iodide uptake plays a key role in the biosynthesis of the thyroid hormones. NIS is also expressed in thyroid cancer (TC) cells. This expression allows the use of radioactive iodide (RAI), which is an important diagnostic and therapeutic tool for malignant and benign diseases, to monitor and eliminate remaining tumor cells and metastases after total thyroidectomy. The lack of response to RAI treatment is due to reduced expression of NIS in TC cells but also to defects in its maturation and targeting to the membrane.

The aim of this project is the construction of a double tagged NIS protein and the assessment of its functional integrity, intended for development of experimental cells systems representative of thyroid non-neoplastic and cancer tissues. These will be engineered to express a fully functional NIS protein containing the triple-HA tag and a fluorescent CFP-tag, while preserving the integrity of the C-terminal regulatory elements. Through this strategy diverse cellular systems can be compared despite having distinct levels of endogenous NIS expression, and potential interferences resulting from NIS transcriptional regulation are avoided.

In this project, three CFP-tagged NIS-HA constructs were generated and compared with respect to their functionality. The presence of the CFP tag allowed the detection of NIS subcellular localization by fluorescence microscopy. These newly synthetized constructs were further specifically detected at the cell surface of intact cells. The results of this work provided a useful tool to investigate how NIS is regulated and retained at the cell surface. Understanding these mechanisms will ultimately allow the development of novel therapeutic approaches to enhance the iodide uptake and RAI efficacy.

Keywords: Sodium/iodide symporter (NIS); Radioactive iodide (RAI) treatment; Gene cloning; Immunofluorescence;

Sumário

O simportador de sódio/iodo (NIS ou SLC5A5) é uma glicoproteína membranar que medeia o transporte ativo de iodo da corrente sanguínea para as células foliculares da tiroide. Este transporte é essencial na biossíntese das hormonas da tiroide, tri-iodotironina (T_3) e tiroxina (T_4), hormonas que controlam o metabolismo e têm um papel muito importante no desenvolvimento neurológico fetal e das quais o iodo é um constituinte fundamental.

O iodo em circulação no sangue entra nas células foliculares da tiroide, passando depois para o lúmen folicular, onde é oxidado e incorporado na tiroglobulina (Tg) por ação da tiroide peroxidase (TPO) em conjunto com o peróxido de hidrogénio (H_2O_2) que é produzido através da ação da dual-oxidase 2 (DUOX2). Este processo de incorporação do iodo é chamado de "organificação", que resulta na formação de mono- e diiodotirosina (MIT e DIT). Assim o iodeto está covalentemente ligado nas posições 3 e 4 dos resíduos de tirosil da Tg e estes resíduos iodinizados são usados para a síntese das hormonas da tiroide. A Tg iodinizada é depois armazenada no lúmen folicular, sendo internalizada e clivada proteoliticamente nos lisossomas, sendo assim libertadas as hormonas T_3 e T_4 na corrente sanguínea. A hormona estimuladora da tiroide (TSH) regula o transporte de iodo para a tiroide. Esta hormona é produzida na adeno-hipófise e é regulada pela hormona libertadora de tireotrofina (TRH) e pelo nível circulante das hormonas da tiroide, havendo um feedback negativo, já que as hormonas da tiroide inibem a produção de TRH. Por outro lado, uma quantidade excessiva de iodeto nas células foliculares pode inibir o transporte de iodo e de "organificação", inibindo o NIS e a TPO. A diminuição das concentrações de iodo pode levar ao aparecimento de desordens de deficiência de iodo (IDD´s), que constituem um sério risco de saúde mundial.

O NIS é uma proteína que é bastante regulada ao nível da transcrição, quer ao nível epigenético, quer ao nível pós-transcripcional, especialmente em relação à sua localização celular. A sua expressão e localização é controlada pela TSH e pelo iodo, sendo promovida pela TSH e inibida pelo excesso de iodo. Esta proteína também está sujeita a bastantes modificações pós-transcripcionais, como fosforilações e sumoilações, e apresenta vários motivos ligados à interação entre proteínas, nomeadamente na sua porção C-terminal. Estes motivos são muito importantes na localização do NIS na membrana celular das células foliculares da tiroide. As citoquinas também mostram ter um papel fundamental na modulação da função do NIS nas células da tiroide, podendo afetar a função da glândula e o seu crescimento, bem como o estradiol, que mostrou ter um papel crucial na modulação do NIS. Este é responsável pelo aumento da glândula da tiroide e pela reduzida expressão do gene do NIS. Hormonas e fatores de crescimento também afetam a expressão de NIS nas células da tiroide. O NIS também é expresso em células cancerígenas da tiroide, sendo esta a neoplasia endócrina mais frequente. No entanto, neste tipo de neoplasia a expressão de NIS funcional encontra-se diminuída, uma vez que a regulação transcripcional e pós-transcripcional do NIS envolve vias de sinalização que também estão implicadas na progressão e agressividade tumoral e que se encontram ativadas neste tipo de malignidades. Entre estas vias de sinalização destacam-se a MAPK/ERK e a PI3K/AKT/mTOR.

O cancro da tiroide pode derivar dos componentes foliculares e parafoliculares da glândula da tiroide, sendo a cirurgia o principal tratamento, independentemente do subtipo histológico. Dentro do subtipo folicular de carcinomas da tiroide, existem 3 categorias no que diz respeito ao seu nível de diferenciação: bem diferenciados (well differentiated thyroid carcinoma - WDTC), pouco diferenciados (poorly differentiated thyroid carcinoma - PDTC) e anaplásicos (anaplastic thyroid carcinoma - ATC). Os WDTC podem ser do subtipo papilar (papillary thyroid carcinoma - PTC) ou folicular (follicular

thyroid carcinoma – FTC). Os WDTC são caracterizados por ter um prognóstico favorável devido à eficácia combinada da cirurgia e do uso de iodo radioativo (RAI). O RAI, é uma importante ferramenta de diagnóstico e terapêutica para doenças malignas e benignas, para monitorizar e eliminar células cancerígenas remanescentes, bem como metástases após tiroidectomia total. A falta de resposta ao tratamento por RAI deve-se a defeitos na maturação, transporte para a membrana e expressão do NIS em células cancerígenas da tiroide, o que leva a uma diminuição no transporte de iodo nestas células. Várias tentativas têm sido feitas com vista a aumentar a expressão de NIS através da manipulação das vias de sinalização do MAPK/ERK e PI3K/AKT. Por exemplo, o uso de inibidores, como o Selumetinib levou a um aumento da captação de RAI em lesões refratárias ao iodo de doentes com cancro da tiroide. Outros inibidores também têm sido usados, como inibidores de cinases e agentes desmetilantes, no entanto com pouco sucesso, uma vez que estas tentativas se focam essencialmente no aumento da expressão do NIS. No entanto, o transporte do NIS para a membrana está diminuído em vários modelos de cancro da tiroide, até em casos em que os níveis de mRNA estão normais ou mesmo aumentados. Isto significa que o processamento pós-transcripcional do NIS, bem como o seu transporte e retenção na membrana é muito importante na eficiência da terapia com RAI. O NIS também é expresso noutros tecidos, incluindo células salivares, nos enterócitos intestinais, na placenta e no tecido mamária durante a lactação, bem como em células de cancro da mama. De facto, cerca de 80% dos carcinomas da mama também expressam NIS, mas a níveis muito baixos para justificar o tratamento com RAI. No entanto, tem sido proposto que caso fosse possível aumentar a expressão funcional de NIS nestes tumores, o uso de RAI como uma terapia coadjuvante seria provavelmente benéfico para muitos pacientes. Por isso, é importante o aumento da abundância e estabilidade do NIS na membrana, em vista a melhorar a captação de RAI.

O objetivo deste projeto é o desenvolvimento e avaliação da integridade funcional de uma proteína NIS marcada com duas marcas peptídicas: uma localizada num domínio extracelular (a marca HA tripla) que permita a deteção específica do NIS na superfície celular, bem como uma marca fluorescente (marca CFP) na sua porção C-terminal citoplasmática, que permita a monitoração da sua localização subcelular durante o seu trafego membranar. A construção destas proteínas NIS marcadas visa o posterior desenvolvimento de sistemas celulares experimentais representativos de tecidos neoplásicos e não neoplásicos da tiroide. Através desta estratégia vários sistemas celulares podem ser comparados. Isto permitirá o estudo do impacto de várias vias de sinalização representativas da progressão e agressividade tumoral no transporte e retenção do NIS na membrana plasmática, bem como a validação de alvos moleculares para o aumento da expressão de NIS funcional e o aumento da captação de iodo.

Neste trabalho, foram desenvolvidas três construções da proteína NIS contendo a marca peptídica HA extracelular (NIS-HA) e a marca peptídica CFP em diferentes localizações do domínio citoplasmático, na tentativa de preservar os elementos regulatórias da porção C-terminal do NIS: NIS-HA-CFP, NIS-HA-CFP-Cter, NIS-HA-CFP-pre-Cter. Estas construções proteicas permitiram a deteção específica do NIS na superfície celular de células intactas e a deteção específica do mesmo, desde a sua biossíntese até ao seu transporte e retenção na membrana plasmática, através de ensaios de biotinilação de proteínas de superfície e microscopia de fluorescência. O NIS-HA-CFP parece ser, entre as construções sintetizadas, o que apresenta uma maior expressão. Também é importante referir que o NIS-HA-CFP apresenta uma distribuição celular distinta, quando comparada com as outras construções, estando mais acumulado na região perinuclear, enquanto o NIS-HA-CFP-Cter se encontra em regiões definidas na periferia celular. Também observámos que a marcação na superfície celular das construções CFP-tagged era menor do que no NIS-HA (sem marca CFP). No que respeita a marcação na superfície celular, as construções NIS-HA-CFP e o NIS-HA-CFP-Cter apresentaram uma forte marcação,

enquanto que a da construção NIS-HA-CFP-pre-Cter, revelou-se fraca. Serão necessários estudos subsequentes para avaliar a capacidade funcional de cada uma destas construções, nomeadamente, a sua capacidade de importe de iodo através de ensaios de influxo de iodo. Este trabalho poderá contribuir para uma melhor compreensão dos mecanismos subjacentes à expressão do NIS, ao serem usados como repórteres do NIS endógeno tanto em células normais como em células cancerígenas. Serão assim usados no estabelecimento de linhas celulares e para o teste de alvos moleculares que possam levar ao aumento da expressão membranar de NIS e o consequente aumento da captação de RAI. Isto poderá contribuir para o desenvolvimento de estratégias que visem a melhoria da eficiência da terapêutica com RAI, que poderão se aplicadas ao carcinoma da tiroide refratário ao iodo ou mesmo a outras condições malignas, não-tiroideias, como é o caso do carcinoma da mama.

Palavras-chave: Simportador de sódio/iodo (NIS); Iodo; Tratamento com iodo radioativo (RAI); Clonagem; Imunofluorescência

Index

Figures Index

Tables Index

List of Abbreviations and Acronyms

AKT	v-akt murine thymoma viral oncogene homolog
ATF-1	activating transcription factor-1
ATC	anaplastic thyroid carcinoma
BC	breast cancer
BRAF	B-Raf proto-oncogene, serine/threonine kinase
B-ZIP	basic-leucine zipper
cAMP	cyclic AMP
C cells	parafollicular cells
CFP	cyan fluorescent protein
CKI	casein kinase I
CKII	casein kinase II
CRE	cAMP responsive element
CREB	cAMP-responsive element binding protein
CREM	CRE-modulator
ddNTP´S	dideoxynucleotides
DIT	diiodotyrosines
DMEM	Dulbecco´s modified Eagle medium
DNA	deoxyribonucleic acid
DPBS	Dulbecco´s phosphate- buffered saline
DTC	differentiated thyroid cancer
DTT	dithiothreitol
DUOX2	dual oxidase 2
ECL	enhanced chemiluminescence
EDTA	ethylenediamine tetraacetic acid
ERK	extracellular regulated MAP kinase
FBS	fetal bovine serum
FTC	follicular thyroid carcinoma
GAP's	GTPase-activating proteins
GDNF	glial-derived neurotrophic factor
GEF's	guanine nucleotide exchange factors
GPCR's	G protein-coupled receptors
HEK293	human embryonic kidney 293 cells
HRP	horseradish peroxidase
IDD´s	iodide deficiency disorders

IFN-γ	interferon γ
IkB	inhibitor of kB
IKK	IkB kinase
IL-1α	interleucin 1α
IL-1β	interleucin 1β
IL-6	interleucin 6
IL-8	interleucin 8
ITD´s	iodine transport defects
MAPK	mitogen-activated protein kinase
MEK	mitogen activated protein (MAP)/ERK kinase
MIT	monoiodotyrosines
MMP´s	matrix metallopepptidases
mRNA	messenger ribonucleic acid
MTC	medullary thyroid carcinoma
mTOR	mammalian target of rapamycin
Na^{+}/K^{+} -ATPase	sodium/potassium pump
NF-κB	nuclear factor kappa-light-chain-enhancer of activated B cell
NIS	sodium/iodide symporter
NIS-HA	NIS with a triple HA protein tag in its 4th extracellular loop
NIS-HA-CFP	NIS-HA with a CFP downstream of its cytoplasmic tail
NUE	NIS upstream enhancer
PAX8	paired box gene 8
PBF	PTTG1-binding factor
PBS	phosphate buffered saline
PBST	phosphate buffered saline with triton
PBS-CM	phosphate buffered saline with $CaCl_2$ and $MgCl_2$
PCNA	proliferating cell nuclear antigen
PCR	polymerase chain reaction
PDTC	poorly differentiated thyroid carcinoma
PDK1	3-phosphoinositide-dependent kinase-1
PFA	paraformaldhyde
PIK3C A	phosphoinositide-3 kinase catalytic α
PIK3C B	phosphoinositide-3 kinase catalytic β
PKA	protein kinase A
PKC	protein kinase C
PPARγ	peroxisome proliferator-activated receptor
PTC	papillary thyroid carcinoma

PTC-FV	follicular variant of PTC
PTEN	phosphatase and tensin homolog
PTTG1	pituitary tumor-transforming gene-1
PVDF- membrane	polyvinylidene fluoride membrane
PI3K	phosphatidylinositol 3-kinase
RAC1	RAS-related C3 botulinum toxin substrate 1
RAC1b	splice variant of RAS-related C3 botulinum toxin substrate 1
RAF	raf-1 proto-oncogene, serine/threonine kinase
RAI	radiodide
RAS	rat sarcoma virus oncogene
Ref-1	redox effector factor-1
RET/PTC	rearrangement of the RET oncogene
RPMI	Roswell Park Memorial Institute 1640 Medium
RTK	receptor tyrosine kinase
SDS-PAGE	sodium dodecyl (lauryl) sulfate-polyacrylamide gel
SLC5	solute carrier family 5
SLC5A5	solute carrier family 5 member 5
SOC medium	super optimal broth with catabolite repression medium
SSS	superfamily of sodium/solute symporters
TBE	tris-borateEDTA
TBG	T_4 binding globulin
TBST	tris-buffered saline with triton
TC	thyroid cancer
Tg	thyroglobulin
TGFβ	transformation growth factor β
TNF-α	tumor necrosis factor α
TNF-β	tumor necrosis factor β
TPC-1	thyroid papillary carcinoma cells
TPO	thyroid peroxidase
TRH	thyrotropin releasing hormone
TSH	thyroid stimulating hormone
TSHR	thyroid stimulating hormone receptor
T_3	triiodothyronine
T_4	thyroxine
USF-1	upstream transcription factor-1
WDTC	well differentiated thyroid carcinoma

1.Introduction

1.1 Thyroid gland

The thyroid gland is located in the lower part of the anterior neck, at the level of the second to third tracheal rings, inferior to the larynx. It is a shield-shaped organ, named after the thyroid cartilage of the trachea (Braverman L.E. et al.,2012). It consists of two lobes, each on the corresponding side of the tracheal wall (Fig. 1.1). They are connected with a thin strip of thyroid tissue that extends across the anterior surface of the trachea called the isthmus (De Felice M. et al.,2011). It is very important in several regulation functions like the metabolic rate, energy expenditure and in the function of several organs like the heart or brain (Rosenberg S.M. et al.,2015).

The thyroid is formed from a midline anlage in the pharyngeal floor consisting of foregut endoderm cells that are committed to a thyroid fate. These cells then give rise specifically to the follicular cell lineage that eventually will form hormone producing units – the thyroid follicles. Differentiated cells within these follicles, known as thyrocytes, are strictly epithelial. Are these cells that produce the thyroid hormones triiodothyronine and thyroxine (T3 and T4), which are iodinated dipeptides that are synthesized, stored and secreted in a complex series of reactions (Rousset et al.,2015). The thyroid also contains a second population of hormone producing cells named parafollicular cells (C cells). These are neuroendocrine thyroid cells whose principal function is to secret calcitonin. Additionally, the thyroid gland contains a vast network of capillaries surrounding each follicle that provides systemic delivery of released hormones (Kameda et al.,2007). The thyroid also contains other interstitial cells such as macrophages and mast cells (Visciano et al., 2015).

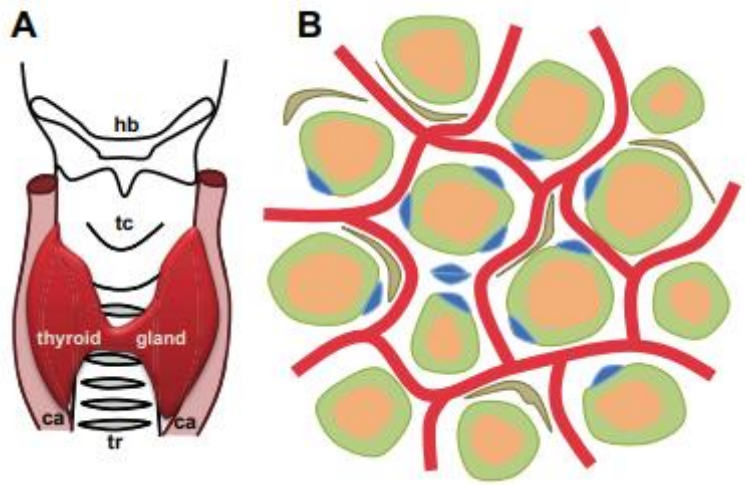

Figure 1.1 – Structure and function of the thyroid gland. (A) The human thyroid gland (red) consists of two lateral lobes and a connecting isthmus portion that crosses the midline at the level of the first or second tracheal cartilaginous rings. hb, hyoid bone; tc, thyroid cartilage; tr, trachea; ca; carotid artery. (B) Follicles, the functional units of the gland, vary in size and shape. Follicular cells (or thyrocytes), the major cell type in follicles, form a monolayered epithelium (green) that encloses a central cavity or lumen filled with colloid (orange), which constitutes a thyroid hormone reservoir. Each follicle is surrounded by a network of capillaries (red). Neuroendocrine cells (or C cells; blue), fibroblasts (grey) and other stromal cells (e.g. macrophages and mast cells; not shown) reside close to the follicles or interstitially (adapted from Nilsson, M. and Fagman, H., 2017).

1.2 Role of iodine in thyroid´s function and regulation of iodide uptake

Iodine is an essential element needed for the production of thyroid hormones, which controls metabolism and plays a major role in fetal neurodevelopment. Its ionized form is called iodide. Iodine deficiency results in impairment of thyroid hormone synthesis and may lead to several undesirable consequences. The impact of iodine deficiency is most significant during fetal life and early childhood development, with manifestation of goiter, delayed physical development and impaired mental function. Adults can manifest impaired mental function, hypothyroidism, and goiter (Zimmermann M.B.,2009).

Iodide (I^-) is transported across the cell membrane by the sodium/iodide symporter (NIS), a plasma glycoprotein that mediates transport of iodide into all iodide-concentrating tissues including the thyroid gland, intestine, salivary gland, lactating breast, and stomach (Dai et al.,1996). The cell´s uptake of iodide mediated by NIS requires an electrochemical sodium gradient from outside to inside of cells, which is maintained by the sodium/potassium pump (Na+/K+ ATPase) (Fig. 1.2). NIS concentrates iodide 30- to 60-fold, relative to the concentration in the blood, into the thyroid follicular cells (Kaminsky et al.,1994). Iodide in the follicular cell then moves into the follicular lumen. Iodide, after translocation into the follicular lumen, is oxidized and incorporated into thyroglobulin (Tg) by thyroid peroxidase (TPO), with hydrogen peroxide (H_2O_2) produced through the action of dual oxidase-2 (DUOX2). This process of incorporation of iodide into protein is called “organification” and results in the formation of mono- and diiodotyrosines (MIT and DIT). Iodine is covalent bound at the 3 and 4 positions of tyrosyl residues on Tg and the iodinized thyroid residues are used for thyroid hormone synthesis. Iodinated Tg is stored in the follicular lumen and it is internalized via endocytosis or micropinocytosis, followed by proteolytic cleavage in the lysosomes with subsequent release of T3 and T4 into the bloodstream (Bizhanova and Kopp,2009).

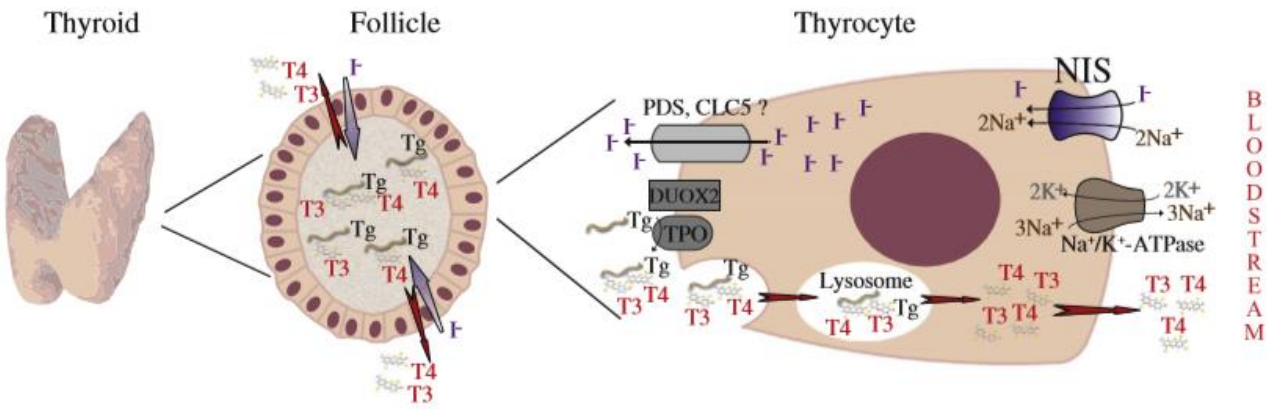

Figure 1.2 – Schematic representation of iodide metabolism in the thyroid. NIS uses the sodium gradient generated by the Na+/K+-ATPase to actively transport iodide into thyrocyte cells. The iodide ions cross the cells and are organified (covalently linked) inside the thyroid follicles by thyroid peroxidase (TPO) onto thyroglobuline tyrosine residues. These iodotyrosines are then coupled to form thyroid hormones. After endocytosis, the iodinated Tg is proteolysed, and the thyroid hormones are released into the bloodstream. (adapted from Elisabeth Darrouzet et al., 2014).

Thyroid stimulating hormone (TSH) regulates iodide transport into the thyroid folicula (Kogai, T. et al.,2006). It is a peptide hormone produced in the anterior pituitary gland (adenohypophysis). TSH is under the regulation of both thyrotropin-releasing hormone (TRH), which is produced in the hypothalamus, and the circulating levels of thyroid hormone (Fig. 1.3). This is a classical feedback loop, frequently described in various endocrine axes. Thyroid hormone inhibits TRH production. This leads

to decreased TSH synthesis and release from the pituitary gland and, in turn, decreased stimulation of the thyroid gland to uptake iodine and synthesize and release thyroid hormone (Ross D.S. et al.,1990).

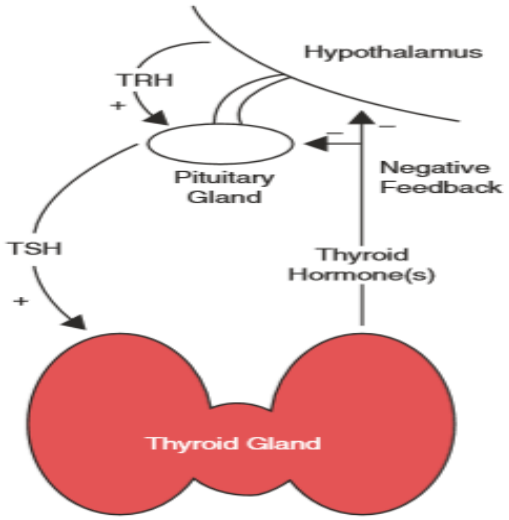

Figure 1.3 - Hypothalamic-pituitary-thyroid axis: negative feedback loop. (adapted from Stathatos, N., 2019).

Conversely, the presence of excess amounts of iodine in the follicular cells can inhibit the process of iodine uptake and organification by inhibiting the NIS and TPO. This inhibition, which is called the "Wolff- Chaikoff" effect, is temporary and results in the depletion of intracellular iodine which, in turn, allows for the reset of the organification mechanism and synthesis of new thyroid hormone.

1.3 Thyroid Cancer

Thyroid cancer (TC) is the most frequent endocrine neoplasia, and its incidence has been rapidly increasing worldwide. The papillary histotype is the most frequent. (Fig. 1.4). TC can derive from both the follicular and the parafollicular components of the thyroid gland. The primary treatment for thyroid carcinoma is surgery, regardless of the histological subtype. Three malignant lesions may derive from follicular cells in what concerns the level of differentiation: well-differentiated (WDTC), poorly differentiated (PDTC) and anaplastic (ATC) thyroid carcinomas. WDTC´s are either papillary (PTC) or follicular (FTC) subtypes. These two types are characterized by specific histological features, and by the maintenance of some differentiating features (Kondo et al.,2006). WDTCs have a favorable prognosis thanks to the efficacy of combined surgical and radioiodine-based therapy, the systemic treatment of choice for WDTC metastatic disease. PDTC´s and ATC´s, which are thought to derive from pre-existing differentiated tumors, show poor or even no accumulation of radiodide and respond poorly to medical and surgical treatment (Rosai et al.,1992). Medullary thyroid carcinoma (MTC), which arises from the parafollicular C-cells of the thyroid, is not a candidate for radiodide therapy, because it does not express NIS. (Roman et al.,2009). So, it will not be a study theme in this thesis.

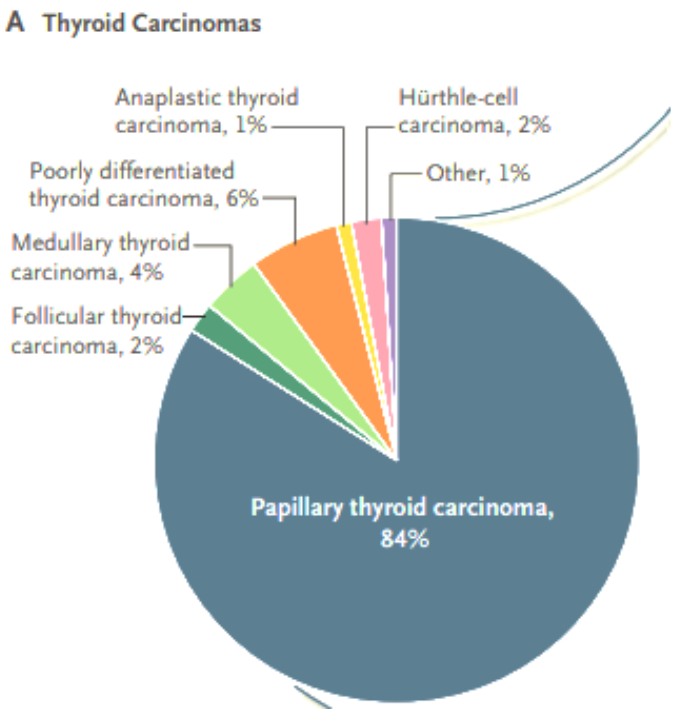

Figure 1.4 – Thyroid Carcinomas. (A) shows the relative incidence of the main types of thyroid cancer in the United States (adapted from Fagin, J.A and Wells, S.A., 2016).

Non-overlapping mutations of RAS and BRAF genes as well as RET-PTC rearrangements are found in about 70% of PTCs. These encode activators of the mitogen-activated protein kinase (MAPK) cascade. RET encodes the tyrosine kinase receptor of growth factors belonging to the glial-derived neurotrophic factor (GDNF) family (Manie et al.,2001). RET/PTC rearrangements are thought to be early events in thyroid tumorigenesis since they are very frequent in clinically silent small PTC (Fusco et al., 2002). Activating point-mutations in RAS small GTPases are found mainly in the follicular variant of PTC (PTC-FV) (Zhu et al.,2003). Point mutations in BRAF are the most common genetic lesion in these tumors (Kimura et al., 2003; Xu et al.,2003; Soares et al.,2003; Cohen et al.,2003).

BRAF is a member of the RAF family of serine/threonine kinases, and it is a component of the MAPK signalling module. FTCs are characterized by RAS point-mutations (Nikiforova et al.,2002) or by the PAX8/PPARγ rearrangement (Kroll et al., 2000). PDTC and ATC can derive from pre-existing WDTCs. RAS point-mutations and the BRAF V600E mutation are prevalent in PDTC and ATC (Garcia-Rostan et al.,2003; Nikiforova et al.,2003; Begum et al.,2004). Finally, p53 mutations are often found in ATC (Donghi et al., 1993; Fagin et al.,1993) (Fig. 1.5).

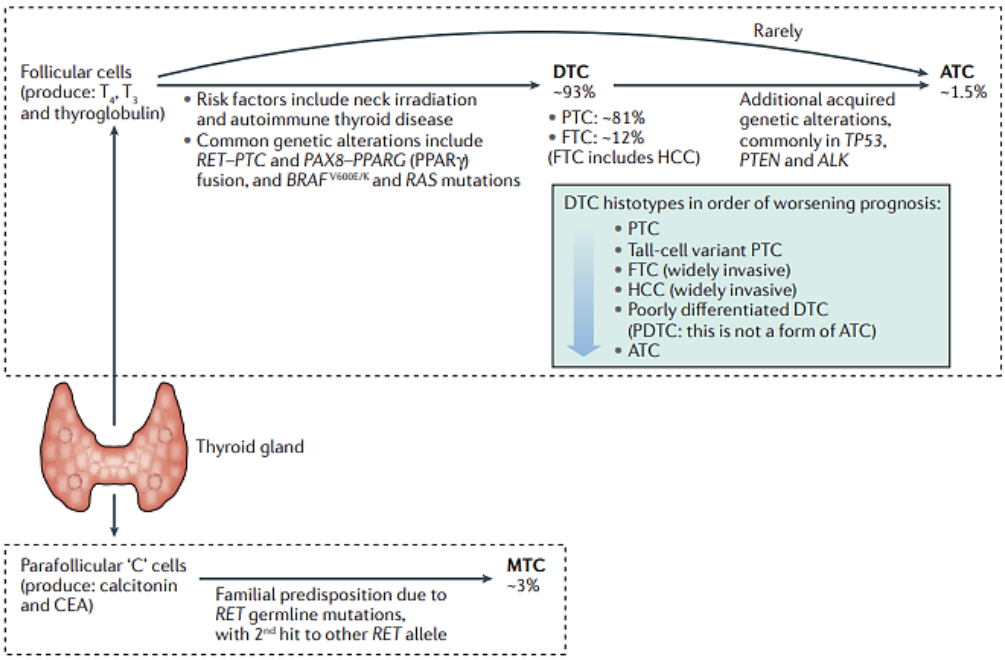

Figure 1.5 – Histological classifications of thyroid cancers. Thyroid cancer histotypes are outlined, along with their cells of origin, contributing aetiological factors, primary genetic alterations, and relative incidence. The relative prognosis of well differentiated thyroid cancer (WDTC) subsets is also shown. ATC, anaplastic thyroid cancer; CEA, carcinoembryonic antigen; FTC, follicular thyroid cancer; HCC, Hürthle-cell carcinoma; MTC, medullary thyroid cancer; PPARγ, peroxisome proliferator-activated receptor γ; PTC, papillary thyroid cancer; T3, tri-iodothyronine; T4, tetraiodothyronine (thyroxine). (adapted from Keith C. Bible1 et al., 2016).

1.4 Radioactive iodine therapy

Radiodide (RAI) is widely used in patients with differentiated thyroid cancer for ablation of residual lesions or metastases after total thyroidectomy. If the RAI uptake is observed in distant metastases, RAI treatment is highly effective and markedly increases the survival rate **(**Durante et al., 2006).

More than 70% of differentiated thyroid cancer, including the papillary and follicular subtypes, expresses NIS and actively uptake RAI. The de-differentiation of thyroid cancer, however, influences the regulation of NIS and reduces functional NIS expression (Kogai, T. et al.,2006). As a result, the tumor is visualized on a radioiodide imaging study as a relatively "cold" nodule with reduced tracer uptake, compared to the surrounding normal tissue. Differentiated thyroid cancer usually retains expression of the TSH receptor (TSHR), although less differentiated thyroid cancer has reduced expression of TSHR (Ohta et al.,1991; Mizukami et al.,1994). The majority of WDTC respond to TSH stimulation with an increase in endogenous NIS expression and RAI accumulation. This stimulation is achieved after total thyroidectomy by increasing serum TSH level through the withdrawal of thyroid hormone treatment, which increases secretion of endogenous TSH from the pituitary due to reduced feedback of circulating thyroid hormone.

The resulting hypothyroidism however may not be well tolerated in some patients and the administration of recombinant human TSH is utilized as an alternative and has similar efficacy to T4 withdrawal, but without significant side effects (Ladenson et al.,1997; Haugen et al.,1999).

In the normal thyroid, the retention time of organified iodine in follicles is significantly longer than that in TC (Wolff et al.,1959; Valenta,1966; Field et al.,1973). Nevertheless, RAI therapy is very effective in patients with DTC (differentiated thyroid cancer), even without extensive organification.

However, a significant fraction of metastatic thyroid cancer, in the range of 30–40%, does not respond to RAI therapy, even in the presence of an elevated TSH (Maxon & Smith,1990). Greater NIS expression in TC is associated with greater uptake of radioiodide (Castro et al.,2001), as well as a better prognosis (Ward et al.,2003). Increased NIS function is desired to improve the efficacy of RAI. The regulation of NIS functional expression in thyroid follicular cells and thyroid cancer cells, has therefore, been intensively studied.

1.5 Sodium/Iodide Symporter (NIS) expression, structure and functional characterization

NIS or solute carrier family 5 member 5 (SLC5A5) is a glycosylated intrinsic membrane protein (De La Vieja, A. et al.,2000 and Jung, H., 2002) with 13 trans-membrane domains (Fig. 1.6). The protein is found in the basolateral membrane of thyroid follicular cells where it mediates efficient iodide uptake from the bloodstream into the thyroid using the sodium gradient generated by $NA^{+/}K^{+}$ -ATPase. It makes an essential contribution to thyroid hormone synthesis and, therefore, to the control of human metabolism in general. NIS is a key protein in thyroid regulation and its expression is finely tuned at the transcriptional levels (Dohan et al.,2003; Kogai, T. and Brent, G.A., 2012). Its function also plays a crucial role in the diagnosis and treatment of benign and malignant thyroid diseases (Riesco-Eizaguirre, G. et al.,2007; Carvalho, D.P. et al.,2007; Hingorani, M. et al.,2010). Studies are currently underway to better control NIS regulation, which could be useful in RAI treatment, since NIS expression in TC is low and radioiodine uptake needs to be enhanced (Ho, A.L et al.,2013).

NIS expression is also found in other cells/tissues, albeit at levels exceedingly lower than thyroid. These include salivary gland ductal cells (Jhiang, S.M. et al.,1998; La Perle, K.M. et al.,2013), lung airway epithelial cells (Fragoso, M.A. et al.,2004), intestinal enterocytes (Nicola, J.P. et al.,2009), epithelial and parietal stomach cells (Kotani, T. et al.,1998), placenta (Bidart, J.M. et al.,2000) and testicular cells (Russo, D. et al.,2011). The functional role of the protein in these tissues remains speculative. Notably, NIS is considerably expressed in breast tissue during lactation (Perron, B. et al., 2001; Tazebay, U.H. et al.,2000; Cho, J.Y. et al.,2000).

NIS belongs to the superfamily of SSS (sodium/solute symporters) in the transporter classification system (Reizer, J. et al.,1994) and to the SLC5 family in the solute carrier nomenclature (Hediger, M.A. et al.,2004; He, L. et al.,2009). Most of the members of these families are symporters and mediate the uptake of a variety of molecules: sugars, amino acids, monocarboxylates, myo-inositol, vitamins, urea and anions (iodide, thiocyanate, perchlorate). Members of the SSS family vary greatly in size, being composed of between 500 and 700 amino acid residues (Jung, H.2002; Wright, E.M. et al.,2004; Wright, E.M.2013). In this family, as for many other symporters, the inward Na^{+} (sodium) gradient and the negative membrane potential drive the transport of the substrates into the cells and several members also behave as uniporters (Eskandari, S. et al.,1997; Wright , E.M.et al.,2004; Loo, D.D. et al.,1999).

NIS transports one iodide ion along with two sodium ions following the inwardly directed sodium gradient. Li^{+} (lithium) can also be used as a coupling cation but the transport activity is only about 10% of that obtained with Na^{+}, while H^{+} (hydrogen) is barely transported (Eskandari, S. et al.,1997). The following anions are known to be NIS substrates: ClO_3^{-} (chlorate), SCN^{-} (thiocyanate),

$SeCN^-$ (selenocyanate), NO_3^- (nitrate), ReO_4^- (perrhenate) and TcO_4^- (pertechnetate) and to a lower extent Br^- (bromide) and BF_4^- (tetrafluoroborate) (Eskandari, S. et al.,1997; Van Sande, J. et al.,2003).

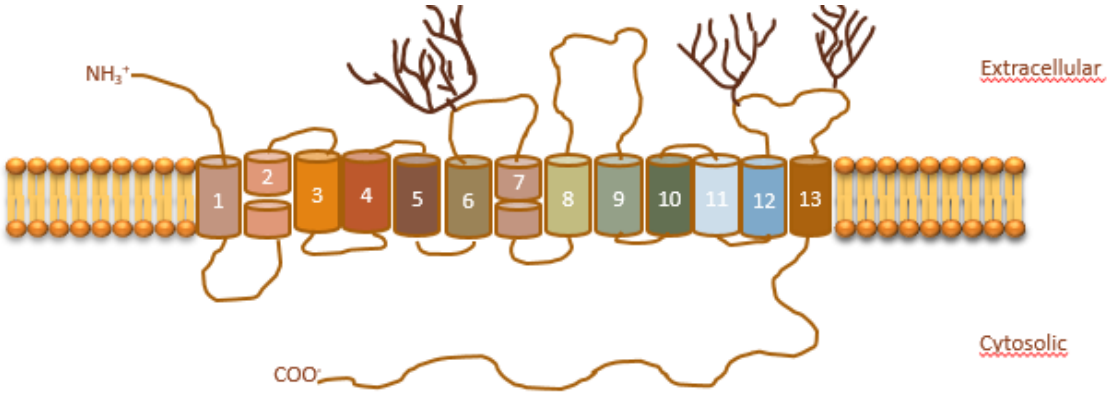

Figure 1.6 – NIS structure model.

NIS is composed of 643 amino acids in humans. The NIS protein carries three N-linked glycosylation's , resulting in a mature protein that migrates at an apparent molecular weight of 80–90 kDa. (Paire, A. et al.,1997; Levy, O. et al.,1998). NIS glycosylation is not required for the correct targeting of the protein to the plasma membrane but plays a role in protein stabilization and folding (Levy, O. et al.,1998).In the latter model, the N-terminus extremity is extracellular and the C-terminus intracellular. The predicted length of the 13 transmembrane segments ranges from 20–28 amino acid residues, except for transmembrane segment V, which contains 18 residues. Only three charged residues are predicted to lie within transmembrane segments, namely Asp 16 in transmembrane segment I, Glu 79 in transmembrane segment II, and Arg 208 in transmembrane segment VI. Of a total of eight Trp residues found in the membrane, six are located near the ends of transmembrane segments close to the putative lipid/aqueous interface (Eskandari S. et al.,1997).

The intracellular C-terminus contains 100 amino acids in the human and represents the longest stretch of amino acid residues predicted to lie outside the membrane. This portion contains numerous potential phosphorylation sites (PKA, PKC, CKII) (Vadysirisack, D.D. et al.,2007). This domain also bears several potential binding sites for regulatory proteins and is predicted by bioinformatics to have few secondary structures, and thus to be intrinsically unstructured. Another feature of membrane proteins, including NIS, is their appearance in different oligomeric forms modulating their maturation, targeting, stability and even function (Veenhoff, L.M. et al.,2002; Sitte, H.H. et al.,2004).

Knowledge of the NIS structure/function relationship has been mainly obtained from studies of NIS gene mutations leading to congenital iodine transport defects (ITD) (S. Faham et al.,2008). Fourteen NIS mutations have been identified in ITD to date. They lead to either the synthesis of truncated proteins (Pohlenz, J. et al.,1997; Pohlenz, J. et al.,1998) proteins with partial deletions (Kosugi, S. et al.,2002; Tonacchera, M. et al.,2003; Liang, J.A. et al.,2005; Montanelli, L. et al.,2009) or amino acid substitutions (Kosugi, S. et al.,2002; Matsuda, A. and Kosugi, S., 1997; Kosugi, S. et al.,1998; Kosugi, S. et al.,1999; Fujiwara, H. et al.,2000; Szinnai, G. et al.,2006) . Some have been further characterized at the molecular level. The V59E mutation causes a complete loss of NIS function (Reed-Tsur, M.D. et al.,2008). It was also discovered that the G93 residue present in TM3 and Trp255,

an amino acid residue in close contact, are implicated in the control of the conformational changes as well as in the stoichiometry (Paroder-Belenitsky, M. et al.,2011). The R124H mutation was also described as a mutation that abolishes NIS iodide uptake activity in cells but does not impair targeting to the membrane (Szinnai, G. et al., 2006). It was also shown that Q267E mutations may lead to an inactive transporter (De La Vieja, A. et al.,2000; De La Vieja, A. et al.,2004). The deletion of amino acid residues 287 and 288, located in TM8, leads to a complete absence of iodide uptake (Montanelli, L. et al.,2009). This region is thus probably also important in NIS for substrate binding/translocation. Analysis of the T354P mutation (Levy, O. et al.,1998) revealed the importance at this position of the hydroxyl group on the threonine beta-carbon for NIS function and led to the finding that other hydroxyl-containing residues surrounding T354 in TM9 are also required for NIS function (De La Vieja, A. et al.,2007). It was also identified amongst several NIS homologues a conserved histidine residue H226. Replacement of H226 by an Ala, Asp, Glu or Lys residue leads to a complete loss of transport activity (Wu, S.L. et al.,2008).

1.6 NIS transcriptional regulation

TSH is the primary regulator of NIS expression in thyroid glands. Stimulation of TSHR activates cyclase trough the Gs-protein, resulting in cyclic AMP (cAMP) accumulation in thyroid cells. The elevation of endogenous cAMP induces NIS transcription by stimulating several signal pathways of cis-regulatory elements in NIS locus (Kogai, T. et al.,2006), including the NIS upstream enhancer (NUE) contained in the NIS promoter (Ohno et al.,1999; Taki et al.,2002).

The human NUE consists of one Pax8 (thyroid-specific transcription factor) binding site and one cAMP-response element (CRE)-like site, both of which are required for the full activity of NUE (Taki et al.,2002) (Fig. 1.7). cAMP stimulates the NUE through both PKA- dependent and -independent pathways in thyroid cells (Ohno et al.,1999; Taki et al.,2002; Chun et al., 2004). PKA phosphorylates the cAMP-responsive element binding protein (CREB) and other basic-leucine zipper (B-ZIP) proteins, such as activating transcription factor-1 (ATF-1) and CRE-modulator (CREM), leading to recruitment of these B-ZIP proteins by the CRE-like element in NUE (Taki et al.,2002; Chun et al.,2004). Pax8 is a key transcription factor for thyroid development and differentiation (Mansouri et al.,1998).

Transcription of thyroid specific genes, including TSHR, Tg, TPO, and NIS, is dependent on PAX8 activity. Binding of PAX8 to the NUE, in response to TSH stimulation (Costamagna et al.,2004), is the primary requirement for significant activation of NUE (Ohno et al.,1999; Taki et al.,2002). The TSH signalling facilitates the reduction of PAX8 (Kambe et al.,1996) through redox effector factor-1 (Ref-1), which stimulates PAX8 binding to its cis-elements (Tell et al.,1998).

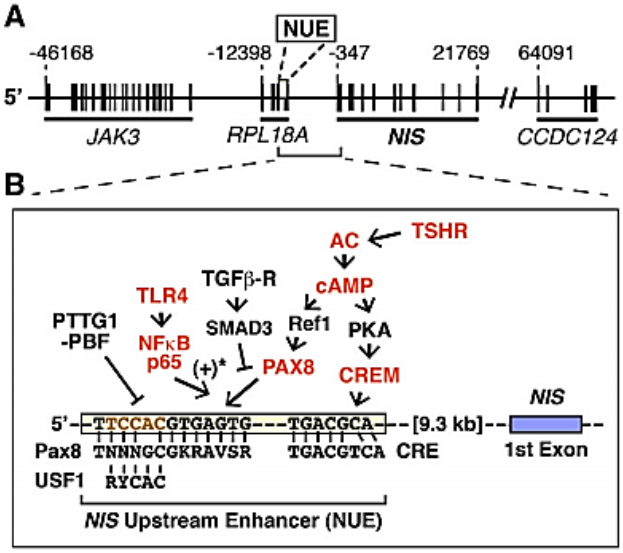

Figure 1.7 - Regulation of the NUE in thyroid cells. (A) Map of the human chromosome 19p around the NIS gene locus. The "A" in the translation start site (ATG) of NIS is referred to as +1. (B) TSHR signalling pathways to NUE. NIS expression in thyroid cells is predominantly regulated by the TSHR signalling to NUE. Gain-of-function studies of the molecules, indicated by red colour, have demonstrated stimulation of the NUE activity. The consensus sequences of cis-elements of PAX8, CRE, and USF1 are indicated along with the sequence of human NUE. *, Stimulatory effects have been reported with rat NUE, which contains an additional Pax8 element and an NFκB element. AC, adenylyl cyclase; Ref-1, apurinic apyrimidinic endonuclease redox effector factor-1 (adapted from Kogai, T. and Brent, G.A., 2012).

Several additional factors have been identified, mostly acting as negative regulators of NIS. The NUE is negatively regulated by the pituitary tumor-transforming gene-1 product (PTTG1) (Fig 1.7) (Boelaert et al.,2007). The cofactor of the PTTG1 is the PTTG1-binding factor (PBF) (Boelaert et al.,2007). The PAX8 element, as well as an overlapping element of upstream transcription factor-1 (USF-1), in the NUE is important for negative regulation by the PTTG1/PBF complex. Abundant expression of PTTG1 (Saez et al.,2006), as well as PBF (Stratford et al.,2005), has been observed in most TC samples, suggesting contribution of those factors to the reduced NIS expression in TC. Also, several in vitro studies have demonstrated that transformation growth factor (TGFβ) suppresses the differentiated function of thyroid cells, including iodide uptake (Pang et al., 1992) and iodide organification (Pisarev et al.,2009).

1.7 NIS post-translational regulation

NIS is a protein that is finely regulated at the transcriptional level, including epigenetic regulation (Kogai, T. and Brent, G.A., 2012; Russo, D. et al.,2011), and at the post-translational level, especially in relation to its subcellular localization. In the thyroid, the protein is located at the basolateral membrane of the follicular cells, whereas for some tissues such as the intestinal epithelium, an apical localization has been described (Nicola, J.P. et al.,2009; Kotani, T. et al.,1998) suggesting that the NIS membrane targeting in polarized cells is cell-type dependent. Under physiological conditions, TSH and iodide control NIS expression and localization to the thyroid plasma membrane, which is promoted by TSH (Paire, A. et al.,1997; Kogai, T. et al.,1997; Riedel, C. et al.,2011) and inhibited by an excess of iodide (Eng, P.H. et al.,1999; Eng, P.H. et al.,2011). The MEK signalling pathway is also important in oncogenic transformation and appears to be a key element in NIS protein stability, at least in breast cancers (BC). Very few data are, however, yet available regarding these processes at the molecular level. Many potential regulation sites that are subject to post-translational modification

(phosphorylation, sumoylation, ubiquitination), or sites of protein/protein interaction (SH3 or SH2 binding motifs, tyrosine-based motifs, PDZ domain protein binding sites…), are present on this protein, mainly at the C-terminal domain. PDZ target motif at the C-terminal tail is one of the sequences involved in protein-protein interactions. PDZ target sequences are recognized by PDZ binding proteins (Fanning, A.S. and Anderson, J.M.,1999). NIS also contains a dileucine motif, which has been proposed to play a role in the sorting of certain membrane proteins within the cell (Tan, P.K. et al.,1998; Dietrich, J. et al.,1997). The dileucine motif, like tyrosine-based sorting signals, interacts directly with the clathrin-coated machinery (Marks, M.S. et al.,1997). This interaction allows for selective incorporation of the integral membrane proteins into coated vesicles that carry proteins to different destinations within the cell. In addition, three acidic dipeptide motifs are present in the C-terminus of NIS. Acidic-based motifs function as retrieval signals for proteins localized at the cell surface (Piguet, V. et al.,1999; Voorhees, P. et al.,1995). Phosphorylation, a common cellular mechanism for modulating activity, subcellular localization, and/or degradation of proteins, is a regulator of the activity of transporters (Glavy, J.S. et al.,2000). NIS contains several consensus sites for kinases, including glycogen synthase kinase 3, cyclin-dependent kinases I (CKI) and CKII, PKA and PKC. NIS is phosphorylated *in vivo* and serines are the main amino acid residues in which phosphorylation occurs, independently of TSH presence (Riedel, C. et al.,1999; Riedel, C. et al.,2001). Although there are some studies about post-translational regulation of NIS, little is known about it.

1.8 Modulators of NIS expression

Cytokines have also been shown to play a role in the modulation of NIS function in thyroid cells. Cytokines can affect thyroid function and growth and cause immunological changes in the gland. These are produced by either infiltrating inflammatory cells or by the thyroid follicular cells themselves in the context of autoimmune diseases (Ajjan, R.A. et al.,1998). The thyroidal effects of cytokines have mostly been examined in FRTL-5 cells kept in TSH-free medium, to which TSH and cytokines were then added simultaneously (Spitzweg, C. et al.,1999). The cytokines investigated include TNF-α, TNF-β, interferon-γ (IFN-γ), IL-1α, IL-1β, IL-6, and TGF-β, all of which exerted an inhibitory effect on thyroid function, including decreased NIS expression and iodine (I^-) uptake.

It has also been proposed that estradiol plays a role in the modulation of NIS. Indirect effects of estradiol on thyroid function include an increase in T4-binding globulin (TBG). An increase in cell growth and the reduced expression of NIS gene are two direct effects of estradiol in thyroid follicular cells. Goiter formation may be promoted by the increase in cell growth and the reduction of NIS gene expression caused by estrogen, which would explain the higher prevalence of goiter in women compared with men (Furlanetto, T.W. et al.,1999).

Hormones and growth factors also exert their effects on thyroid cells and NIS expression, via several signal transduction pathways. The TSH-TSHR-cAMP-PKA pathway has for a long time been considered the central and most important pathway for thyroid cell proliferation and differentiation (Dremier, S. et al.,1997). This pathway has been reported to play a role in the regulation of NIS expression (Ohno, M. et al.,1999). Interestingly, evidences indicate that cAMP pathways, both PKA dependent and independent, contribute to thyroidal cell differentiation and therefore regulation of NIS expression (Kawasaki, H. et al.,1998).

1.9 NIS expression in thyroid cancer

The main reason for impaired iodide uptake in refractory TC is the defective functional

expression of NIS (Spitzweg, C. et al.,2014; Durante, C. et al.,2006). Transcriptional and post-transcriptional regulation of NIS expression involves different molecular players and signalling pathways that are also implicated in tumor progression and aggressiveness. NIS expression levels and iodine uptake in DTC are reduced when compared to normal tissue (Lazar, V. et al.,1999; Espadinha, C. et al.,2009) and this downregulation has been associated with the over activation of several pathways linked to thyroid malignancy (Lakshmanan, A. et al.,2014). Among those stands out the MAPK/ERK and PI3K/AKT/mTOR pathways which have been shown to negatively impact NIS functional expression

- MAPK/ERK pathway:

MAPK/ERK pathway could be activated by receptor tyrosine kinase (RTK), G protein-coupled receptors (GPCR's), and cytokines. It can then transduce extracellular signals into the cells and nuclei to induce biological responses including cell proliferation, differentiation, and apoptosis. Previous studies have demonstrated that increased activation of MAPK/ERK pathway, which is related with mutations of BRAF gene, is generally found in thyroid cancers (Vidal, A.P. et al.,2013; Leonardi, G.C. et al.,2012). These findings have suggested that BRAFV600E variation is closely associated with the development of PTC (Xing, M., 2007) The findings that BRAFV600E variation is associated with pathological features including bigger PTC diameter, multifocality, extrathyroidal invasion, and lymph node metastasis (Lim, J.Y. et al.,2013; Li, C. et al.,2012) have suggested BRAF mutation is closely associated with poor prognosis of PTC (Elisei, R. et al.,2012; Xing, M. et al.,2013; Fernandez, I.J. et al.,2013). MAPK pathway could also be regulated by upstream factors including receptor RAS oncogene, and RAF/ERK protein-serine/threonine kinases (Fig. 1.8).

Numerous studies have reported an association of BRAFV600E with decreased or lost expression of NIS in PTC (e.g. Zhang et al.,2013), while others have shown that introduced expression of BRAFV600E in thyroid cells could induce the silencing of the NIS gene (e.g. Liu et al.,2007). BRAF V600E expression could also cause misallocation of NIS in the cytoplasm in addition to its decreased expression in thyroid cells (Riesco-Eizaguirre et al.,2006). In *in vitro* cell line assays, inhibition of the BRAFV600E/MEK pathway or silencing of BRAFV600E expression could restore the expression of NIS in thyroid cells (Liu et al., 2007), which provided important therapeutic implications for targeting the BRAFV600E/MAPK pathway to restore thyroid gene expression and radioiodine avidity of radioiodine- refractory TC (Fig. 1.9).

In fact, in a trial with the inhibitor, Selumetinib, an increase in RAI uptake was observed in patients with RAI-refractory TC carrying MAPK activating mutation (Ho, A.L. et al.,2013). This illustrates the clinical relevance of targeting these pathways to enhance the efficacy of RAI therapy. However, many other studies using nuclear receptor agonists, inhibitors, demethylation agents and even tumor-targeted NIS gene therapy, have been less successful. In fact, despite of all the achievements in this area, no complete responses or improvement of overall survival have been demonstrated in TC for any tested agent (Spitzweg, C. et al.,2014).

- PI3K/AKT pathway:

PI3K/Akt pathway is a very important intracellular signalling pathway for mammals, which is closely associated with cell proliferation, transformation, metabolism, motility, and development and progression of tumors (Hsieh, A.C.et al.,2011). Activated PI3K/Akt pathway could also activate other pathways including for example NF-κB pathways (Abbosh, P.H.et al.,2005; Burrows, N. et al.,2011;

Guigon, C.J. et al.,2009). PI3K-activated Akt could in turn phosphorylate a series of downstream target proteins including mammalian target of rapamycin (mTOR) to activate or inhibit their functions, which finally promote cell survival. Therefore, Akt has been regarded as an antiapoptotic regulator (Sale, E.M. et al.,2006). mTOR is also a member of PI3K protein kinase family and an important downstream molecular of PI3K pathway. PI3K/Akt/mTOR pathway could induce the development of tumor by promoting cell motility and angiogenesis (Fig. 1.8). RAS mutations are the second most frequent gene alterations in thyroid cancer, which also activates PI3K/Akt pathway (Liu, Z. et al.,2008; Abubaker, J. et al.,2008).Among other genetic alterations impacting the PI3K/Akt pathway include mutations of RTK, RAS, and phosphatase and tensin homolog (PTEN) deleted on chromosome 10 encoding genes, extra copies of phosphoinositide-3 kinase catalytic α (PIK3C A), phosphoinositide-3 kinase catalytic β (PIK3C B), 3-phosphoinositide-dependent kinase-1 (PDK1) encoding genes, and rearrangement of PPARγ/Paχ8 encoding gene (Liu, B. et al.,2012).

Selective inhibitors of PI3K, significantly increase NIS mRNA expression in rat thyroid cells by stimulating its transcription. The PI3K inhibitors have the potential to increase RAI accumulation, (Liu et al.,2007) in some DTC tissues. Kogai, T. et al.,2008 also demonstrated that PI3K inhibition significantly increases iodide uptake in TSH stimulated and non-TSH stimulated FRTL-5 cells. These authors also verified that the effect of PI3K in NIS-expressing human papillary thyroid cancer cells was mimicked by an inhibitor of AKT, hence indicating a contribution of the canonical PI3K/AKT pathway (Fig. 1.9).

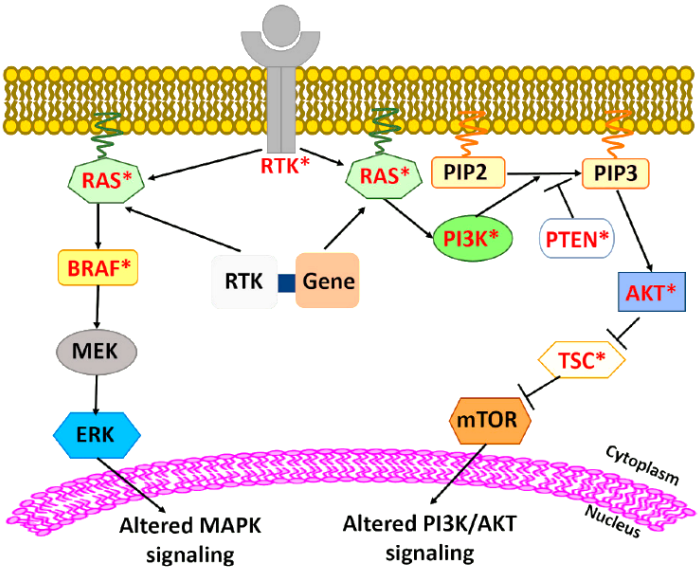

Figure 1.8 - Genetic alterations affecting MAPK/ERK and PI3K/AKT pathway in thyroid cancer. (adapted from Al-Jundi et al., 2020).

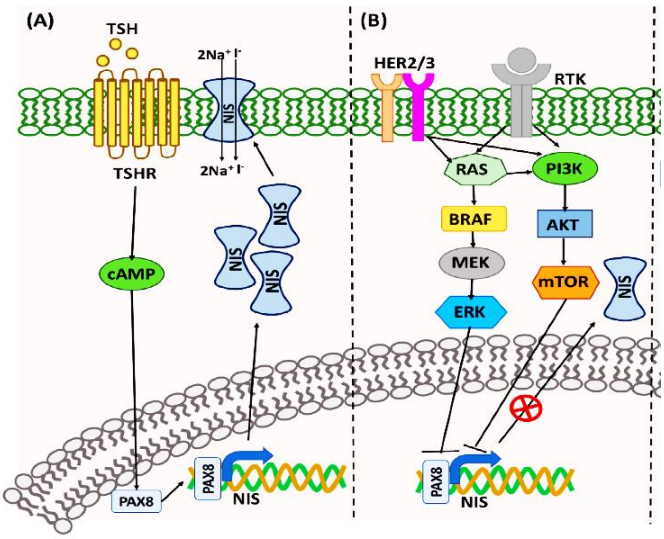

Figure 1.9 – Altered MAPK/ERK and PI3K/AKT pathway affecting NIS expression. (A) Under normal conditions, expression of sodium-iodide symporter (NIS) is regulated through TSHR, resulting in stimulation of thyroid-specific transcriptional factors such as PAX8, wich promotes NIS transcription and its expression on the cell surface. (B) In thyroid tumor cells with hyperactive MAPK/ERK and PI3K/AKT signalling the NIS transcript is repressed, resulting in loss of its cell surface expression and RAI resistance. adapted from Al-Jundi et al.,2020).

- NF-κB signalling pathway:

The association between NF-κB and tumor development mainly relies on the fact that NF-κB could inhibit cell apoptosis (Pacifico, F. and Leonardi, A.,2010; DiDonato, J.A. et al.,2012) Previous studies have demonstrated that NF-κB pathway is activated in several malignancies including TC (Li, X. et al.,2013; Liu, J. and Brown, R.E., 2012). Specifically, for TC, NF-κB activation was found in PTC's, FTC's, and ATC's, and it was suggested that activation of NF-κB could promote dedifferentiation of PTC's and FTC's and thus play important roles in each stage of TC (Li, X. et al.,2013; Liu, J. and Brown, R.E.,2012). BRAFV600E could increase the carcinogenicity of TC cells through NF-κB thus increasing the invasiveness of these cells (Palona, I. et al.,2006; Bommarito, A. et al.,2011). Yamashita et al 2013 suggested that mutations of BRAF and RAS genes and rearrangement of RET/PET gene could activate MAPK pathway, which in turn activate NF-κB pathway and increase the progression and invasiveness of PTCs. NF-κB could regulate the expression of matrix metallopeptidases (MMP's) and IL-8 to allow cancer cells obtain invasiveness, which could then infiltrate surrounding tissues and metastasize to distant organs. Specifically, MMP's could dissolve and damage extracellular matrix and thus increase the infiltration and metastasis of cancer cells (Komorowski, J. et al.,2002) Inhibition of NF-κB activation could affect the growth, apoptosis, and invasion of thyroid cancer cells (Bauerle, K.T. et al.,2010).

Our group also demonstrated that RAC1b, a splice variant of a small GTPase RAC1, which has major importance in signalling cascades that controls cell proliferation, is a potent activator of NF-kB in thyroid tissue (Faria, M. et al, 2017). NF-kB dimers are held in the cytoplasm in an inactive form bound to the specific inhibitor (IkB). In response to stimuli, the IkB kinase (IKK) complex mediates the phosphorylation of IkB, inducing its degradation by the ubiquitin-proteasome pathway. This enables free, active NF-kB dimers to translocate to the nucleus and activate transcription of genes involved in several biological processes such as proliferation, migration and resistance to apoptosis (Xiao, G. et al, 2006). RAC1b was previously shown to act as relevant player in the stimulation of cell cycle progression and cell survival through pathways involving NF-kB (Matos, P. et al,2005).

Interestingly Faria, M et al, (2020) also demonstrated that TNF-α mediated activation of NF-κB downregulates NIS expression in thyroid cells. It was also observed a similar effect when NF-κB activation was triggered independently of ligand-receptor specificity. This study shows that TNF-α downregulation of NIS expression was reverted when NF-κB-dependent transcription was blocked, demonstrating the requirement for NF-kB activity. Additionally, NF-κB was shown to have a negative impact on TSH-induced iodide uptake, consistent with the observed transcriptional downregulation of NIS. These data support the involvement of NF-κB-directed transcription in the modulation of NIS expression, where up- or down-regulation of NIS depends on the combined output of NF-κB activation by several converging pathways.

- RAC1 and RAC1b:

RAC1 is one of the members of the Rho family of small GTPases. Rho stands for RAS homologous and like RAS proteins, functions as molecular switches; they are active in the GTP-bound state and inactive in the GDP-bound state. The switching between the active and inactive forms is controlled by several accessory proteins: guanine nucleotide exchange factors (GEF's), GTPase-activating proteins (GAP's) and GDP-dissociation inhibitory factors. (Symons, M., 1996). RAC1 is a key intervenient in a wide variety of cellular processes, comprising actin remodelling, cell migration and cell cycle progression. (Ridley, A.J. et al.,2003; Vega, F.M. and Ridley, A.J., 2008). RAC1 is also implicated in cancer associated processes, including anchorage-independent growth, cell transformation, survival and invasion (Cerezo et al.2009; Bid et al.,2013; Moshfegh et al.,2014). Under normal conditions RAC1 activity is controlled by the opposing activities of GEFs (which exchange GDP for GTP and activate RAC1), and GAP (which stimulate the conversion of bound GTP to GDP and inactivate RAC1) (Ridley, A.J., 2001).

In 1999, the RAC1 spliced isoform, RAC1b, was described by Jordan and colleagues. This isoform, results from an in-frame insertion of 19 amino acid residues immediately C-terminal to the "switch II" domain (residues 60-76) within the reading frame of the GTPase, due to its 57 additional nucleotides (Matos, P. et al.,2000).These extra nucleotides result from an alternative splicing mechanism, carried out by the spliceosome, a massive structure and a wide number of auxiliary proteins cooperating to accurately recognize the splice sites and catalyse de splicing reaction (Fig.1.10) (Zhou et al.,2013)

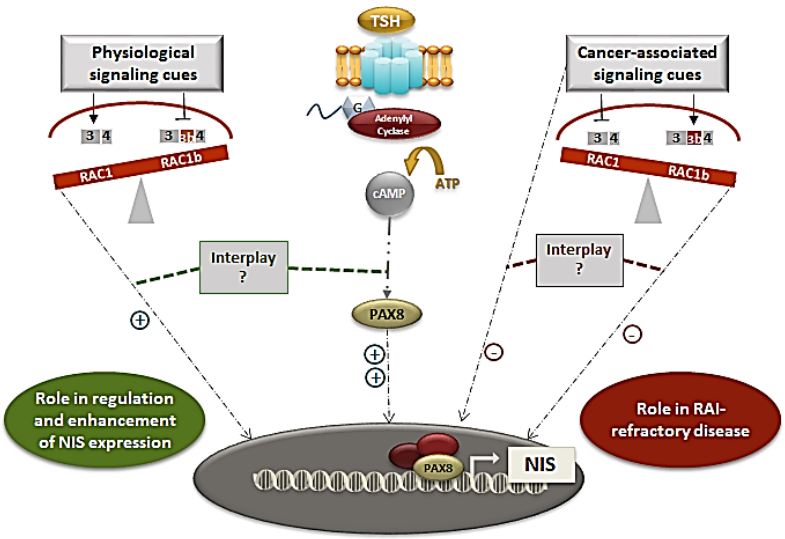

Figure 1.10 - Schematic representation of the antagonistic activities of RAC1 and RAC1b on NIS expression. (adapted from Faria, M. et al., 2019).

Comparably to RAC1, RAC1b presents its self predominantly in a GTP-bound active form, due to an accelerated GDP/GTP exchange activity (Matos, P. et al.,2003). These features render this protein predominantly in its active state, granting it important tumorigenic properties.

In a study by Kogai, T. and Brent, G.A. (2012), using MCF-7 cells, RAC1 was shown to have the ability to stimulate NIS expression. RAC1b, on the other hand, was shown to be overexpressed in a number of papillary thyroid carcinomas, carrying the activating mutation BRAFV600E, with unfavorable outcome (Silva, A.L. et al.,2013). Notably, it was shown that while hyperactive, the RAC1b variant has a very selective downstream signalling (Matos, P. et al.,2003) and may even compete with and inhibit RAC1 endogenous activity in signalling pathways where RAC1b does not participate (Matos, P. et al.,2003). In fact, antagonistic effects of RAC1 and RAC1b on NIS transcriptional regulation have been recently reported by our group (Faria, M. et al 2019).

1.10 NIS in radioiodine treatment

RAI therapy for thyroid diseases relies in the fact that thyroid follicular cells and DTC are more efficient at trapping circulating RAI than other tissues (Ahn, B.C. et al.,2011). RAI treatment has been the most preferred therapeutic approach to hyperthyroidism in the United States of America and it has been one of the key treatments for DTC´s worldwide (Cooper, D.S. et al.,2009; Bahn Chair RS. et al.,2011). However, RAI treatment is not very effective in de-differentiated thyroid cancer, in which NIS expression is downregulated, and is irrelevant in ATC and MTC, which do not express NIS (Verburg, F.A. et al.,2011; Oh, S.W. et al.,2011).

Several attempts have been made in order to increase NIS expression through the manipulation of MAPK/ERK and PI3K/AKT pathways. For example, the use of inhibitors, like Selumetinib, have shown a meaningful increase in RAI uptake in patients with RAI-refractory TC carrying MAPK activating mutations (Ho, A.L. et al, 2013). Other inhibitors have also been used, like nuclear receptor agonists, other kinase inhibitors, histone deacetylase inhibitors, demethylation agents, and even tumor-targeted NIS gene therapy, however with less success (Spitzweg, C. et al,2014). This may be due to the fact that NIS abundance in the plasma membrane is diminished in RAI-refratory TC and due to the fact that the majority of the attempts made are essentially focused on the upregulation of NIS at the transcriptional level (Kogai T. and Brent, G.A. 2012). In fact, NIS membrane targeting was shown to be diminished in several TC models, even in the presence of abundant NIS mRNA levels (Dohan, O. et al,2001; Wapnir, I.L. et al,2003). This means that NIS posttranslational processing, delivery and retention at the membrane is crucial in the efficiency of RAI uptake. However little is known about these processes (Dohan, O. et al,2003) despite knowing that TSH is crucial for NIS posttranslational regulation, by increasing its expression, stability and trafficking. Yet, the molecules mediating these effects remain uncharacterized. In truth, very few putative binding partners of NIS have been reported.

Of note, NIS was found to associate at the plasma membrane with the PBF, which has been implicated in the recruitment of ubiquitin ligase (Read, M.L. et al,2014). Consistent with a role for ubiquitination in the destabilization and internalization of NIS from the plasma membrane, this association was shown play a crucial part in diminished NIS plasma membrane abundance (Piper, R.C. et al,2014; Smith, V.E.et al,2013).

NIS is also expressed in lactating breast, and in 70%-80% of BC (Tazebay, U.H. et al,2000; Poole, V.L. and MacCabe, C.J. et al,2015), however its expression is very low, so the use of RAI is not

effective (Moon DH. et al,2001). Similar of what happen in TC, NIS expression in BC is high in intracellular compartments but low in the plasma membrane (Wapnir, I.L. et al,2003; Kogai T. el al,2004).

In summary, strategies directed to upregulate NIS expression at mRNA/protein level will probably not be effective enough if posttranslational regulation does not promote plasma membrane traffic and retention. Therefore, additional strategies that promote posttranslational stimulation of NIS to enhance the functional expression of the available NIS and increase the efficacy of RAI therapy may be of great clinical relevance in refractory TC. For this, the development of cellular models that allow the evaluation of NIS expression in response to different stimuli is very important, also as the capability of following NIS since its production to its delivery and retention in the plasma membrane.

2. Aims

In order to improve NIS membrane abundance and stability, which could provide an additional level of therapeutic intervention to enhance RAI, the impact of signalling pathways representative of tumor progression and aggressiveness in NIS delivery and retention at the plasma membrane should be addressed. The optimal output for this study will be the successful establishment of tagged-NIS cell lines and assessment of its functional integrity, which will further allow functional validation of molecular targets to enhance NIS functional expression and iodide uptake efficiency.

The present work will focus in the development of experimental cell systems which will further allow functional validation of molecular targets to enhance NIS functional expression and iodide uptake efficiency. Specifically, NIS -expressing cell lines will be established, and its functional integrity will be assessed. These cell systems will be engineered to express a fully functional NIS protein containing the fluorescent CFP (cyan fluorescent protein) tag at its cytoplasmic tail, while preserving the integrity of the C-terminal regulatory elements. This will allow the specific detection of NIS from its biosynthesis to its delivery and retention at the plasma membrane, the comparison of diverse cellular systems, despite having distinct levels of endogenous NIS expression, and will avoid potential interferences resulting from NIS transcriptional regulation.

3. Materials and Methods

3.1 Generation of expression vectors

The plasmid containing the NIS coding sequence was purchased from *Genescript* (pSLC5A5; ID: 6528). The insertion of a triple HA protein tag in the 4th extracellular loop of NIS (NIS-HA), had previously been carried out. NIS-HA coding sequence was then subcloned into PeCFP-N1 expression vector (*Clontech*) (See Appendix Figure 7.1) in order to obtain a construct with the CFP inserted downstream of the cytoplasmic tail of NIS (NIS-HA-CFP). Two additional constructs, NIS-HA-CFP-Cter and NIS-HA-CFP-pre-Cter were subsequently generated from the NIS-HA-CFP backbone.

In order to obtain the several CFP-tagged NIS-HA constructs, NIS-HA coding sequence was amplified by PCR (polymerase chain reaction) using primers with linkers for NheI and HindIII restriction sites (primers: link Nhe 5´ CTAGCTAGCATGGAGGCCGTGGAGACCG and link Hind III 5´ CCCAAGCTTGAGGTTTGTCTCCTGCTGGTC). The C-terminal portion of the NIS-HA was also amplified by PCR using primers with linkers for BsrGI and NotI restriction sites (primers: link BsrGI 5´ GAGCTGTACAAGATCTCCTATCTCTATTACGGTGC and link NotI 5´ GCGGCCGCTCAGAGGTTTGTCTCCTGCTGG). PCR mixes were similar for both amplicons, containing 12,5 µl of PCR master mix from KAPA2G Fast ReadyMix PCR Kit *(KAPABIOSYSTEMS*, KR0374) and 1,25 µl of both forward and reverse specific primers (10 µM), along with 50 ng of plasmid DNA and H_2O up to 20 µl. The thermal cycle profile is depicted in table 2.1.

Table 2.1 – Amplification PCR conditions.

Stage	**Temperature ºC**	**Time**	
Initial denaturation	95 ºC	3 min	
Denaturation	95 ºC	15 s	25 cycles
Annealing	65 º C	15 s	
Elongation	72 ºC	15 s	
Final elongation	72 ºC	4 min	
Inactivation and cooling	4ºC	∞	

For the production of the NIS-HA-CFP protein construct, the PeCFP-N1 vector was digested with the restriction enzymes NheI and HindIII in order to insert the NIS-HA amplified coding sequence. In the NIS-HA-CFP-Cter protein construct, the NIS-HA-CFP construct was used as template. The C-terminal previously amplified was inserted in an intermediate PeCFP-N1 vector, after its digestion with BsrGI and Not I. Then, the NIS-HA-CFP protein construct was digested with HindIII and Not I and the sequence containing the fluorescent CFP-tag and C-terminal was inserted, after being removed from the intermediate PeCFP-N1 vector. To produce the NIS-HA-CFP-pre-Cter, the NIS-HA-CFP protein construct was also used as template. In this case the NIS-HA-CFP protein construct was digested with NheI and HindIII restriction enzymes, and NIS-HA without its C-terminal was inserted in this location. The insertions were made using the QUICK LIGATION™ KIT (*BioLabs*) and the restriction enzymes used were from *ThermoFisher Scientific™*

PCR or restriction products were resolved by electrophoresis on a 1% or 2% (w/v) agarose gel in 1X Tris-borateEDTA (TBE) buffer (diluted from 10X TBE, GB12.0510, *GRiSP Research Solutions*) and stained with 0.05% (v/v) ethidium bromide (See Appendix Table 7.1). DNA fragments were visualized under UV light and image acquired in a gel documentation system (*VWR™*).

Gel-purification of DNA fragments from agarose gels after electrophoretic separation was performed when required using the NZYGelpure Kit (*NZYTech Genes & Enzymes*, MB01102) through the protocol for DNA purification from agarose gels.

Bacterial transformation with the several constructs was performed, using DH5alfa bacteria (*NZYTech Genes and Enzymes*). These are chemically competent E.coli cells engineered to maximize transformation efficiency. For the transformation procedure, 50 µl of competent cells were mixed with 1-5 µl of the plasmid constructs and incubated on ice for 30 min. Then, cells were heat-shocked for 45 seconds at 42ºC followed by a 2 min incubation on ice. Then, 250 µl of SOC medium (super optimal broth with catabolite repression) (*NZYTech Genes and Enzymes*) was added to the bacterial suspension and incubated for 1 hour at 37ºC. After the incubation, 150 µl of the bacterial suspension was plated on LB agar plates using kanamycin as a selection agent (20 ml LB agar + kanamycin (10 µl per plate)). The antibiotic resistant clones were screened by PCR using specific primers. The selected positive clones were then amplified in a LB liquid medium miniculture, with the same antibiotic. Plasmid DNA extraction from minicultures was performed using the Plasmid DNA Minipreps Kit (*Easy Spin*®, SP-PMN).

3.2 Sequencing

Sanger sequencing method was used to confirm the sequence integrity of the constructs generated. For this, 300 ng of each plasmid DNA was mixed with 4 µl of Big Dye (mix with ddNTP´S labelled with fluorescent dyes) (*Apllied Biosystems*™), 0,4 µl of the primer of interest (*ThermoFisher Scientific*™) and H_2O to a final volume of 20 µl. The thermal cycling profile depicted in table 2.2 was used.

Table 2.2 – Sequencing PCR conditions.

Stage	**Temperature ºC**	**Time**	
Initial denaturation	96 ºC	3 min	
Denaturation	96 ºC	10 s	25 cycles
Annealing	50 º C	5 s	
Elongation	60 ºC	4 min	
Inactivation and cooling	4ºC	∞	

3.3 Cell culture and transfection

In the present study, we used the available commercial cell lines HEK293 and TPC-1. These two cell lines are semi-adherent (HEK293) and adherent (TPC-1). The TPC-1 cell line is derived from human papillary thyroid carcinoma and is characterized by having a RET/PTC rearrangement. HEK293 is a non-malignant cell line derived from embryonic human kidney. Both cell lines were maintained at 37ºC in a humidified environment with a 5% CO2 atmosphere. When cells reached confluence of about 80-100%, they were washed with Dulbecco´s phosphate buffered saline 1x (DPBS1x, *Lonza),* detached by incubation at 37ºC, for 1 minute, with 0,05% trypsin-ethylenediamine tetraacetic acid (trypsin-EDTA, *Gibco*) and subcultured in a new flask. HEK293 cells were cultured in Dulbecco´s modified eagle medium (DMEM, *Gibco*) supplemented with 10% (v/v) FBS (fetal bovine serum) and TPC-1 were cultured in RPMI (*Gibco*) supplemented with 10% (v/v) FBS.

Transfections of NIS-HA-CFP, NIS-HA-CFP-Cter and NIS-HA-CFP-pre-Cter were performed using Lipofectamine™ 3000 (*Invitrogen*), according to the manufacturer´s instructions. The PeCFP-N1

empty vector and NIS-HA (without CFP tag) constructs were used as mock controls when appropriate. Just before transfection, cells seeded in 6 or 8 well-plates at 70-80% confluence were fed with new fresh complete DMEM (HEK293) and RPMI medium (TPC-1) and transfected with 2,0 µg and 200 ng of total plasmid DNA, respectively.

3.4 Protein extraction, SDS Page and Western Blotting

Protein extracts were obtained from cell lysates by using laemmli lysis buffer (See Appendix Table 7.2).

The proteins were separated in a sodium dodecyl sulfate-polyacrylamide gel electrophoresis (SDS-PAGE) that consisted in two distinct gels: a lower (resolving) and an upper (stacking) gel (See Appendix Table 7.3). The electrophoresis was carried in 10% polyacrylamide glycerol-containing gels in SDS-PAGE buffer at 150v for 1h. The protein bands were then transferred to a PVDF membrane (polyvinylidene fluoride membrane; *BIO-RAD*), previous activated with methanol, using blot buffer and a blot electrophoresis transfer cell (*BIO-RAD*) for 1.30h at 300mA. Then, membranes were stained with coomassie blue and washed: firstly, with a destain solution and then with tris-buffered saline 0.05% triton x-100 (TBST) (See Appendix Table 7.4). Membranes were blocked in blocking buffer (20 mM Tris–HCl, pH 7.6, 140 mM NaCl, 0,05 % (v/v) Triton X-100, 5% skim milk powder) and probed with primary mouse anti-HA (1:500, *Roche*) or rabbit anti-HA (1:500, *SIGMA*), rabbit anti-GFP (1:2000, *ABCAM)* and mouse anti-PCNA (1:2000, *MERCK*) diluted in TBST Milk. Detection was carried out using HRP-conjugated secondary antibodies (anti-mouse or anti-rabbit, accordingly) diluted in TBST Milk in 1:5000 dilution. The Immunoreactive bands were detected by chemiluminescence using ECL (enhanced chemiluminescence) Western blotting substrate (See Appendix Table 7.4) followed by exposure and image acquisition in Curix 60 (*AGFA HealthCare*).

3.5 Fluorescence microscopy

Analysis and detection of total NIS-HA protein constructs was accomplished by fluorescence microscopy. For this purpose, HEK293 transfected cells were seeded on 8 well µ-Slide (*IBIDI*). Then, cells were washed with PBS 1X (phosphate buffered saline; *Lonza*) and fixed in PFA 4% during 30 minutes at room temperature. Then, cells were permeabilized using PBS with 0,5% (v/v) Triton X during 15 minutes. After this, cells were washed with PBST (PBS+Triton (0,01%)) and stained with phalloidin-TRITC at 1:500 dilution during 30 minutes. For the particular case of NIS-HA (CFP-untagged) detection was performed using mouse anti-HA Ab at 1:100 dilution (*Roche*) for 1h followed by anti-mouse Alexa Fluor 488 secondary Ab at 1:500 dilution (*Thermo Fisher Scientific™*) for 30 min. Then cells were washed with PBST three times and fixated again with PFA 4% during 15 minutes. Images were acquired on a Zeiss widefield fluorescence microscope.

For specific detection of membrane associated NIS-HA protein constructs, HEK293 and TPC-1 cells were gown on 8 well µ-Slide (*IBIDI*). For this purpose, cells were rinsed on ice with cold PBS-CM (PBS, pH 8.0, containing 1 mM $CaCl_2$ and 1 mM $MgCl_2$) and incubated with rabbit anti-HA Ab at 1:100 dilution (*SIGMA*) in PBS-CM for 1 h at 4 °C, without permeabilization. Then cells were washed three times with ice-cold PBS-CM and incubated with anti-rabbit Alexa Fluor 532 secondary Ab at 1:500 dilution (*Thermo Fisher Scientific™*) for 1 h at 4 °C. The cells were again thoroughly washed in PBS and then fixed with 4% formaldehyde for 15 min. Images were acquired on a Leica TCS-SPE confocal microscope.

3.6 Biotinylation

In order to address the residency of proteins derived from different NIS constructs at the plasma membrane of the transfected cells, cell surface protein biotinylation technique was used. Cells were seeded and transfected in six well plates. Twenty-four hours after transfection cells were incubated at 4ºC to pause membrane trafficking and then were washed 3 times with cold PBS-CM. Then, the cells were incubated during 30 minutes with biotin solution (0.5 mg/mL in PBS-CM). After that, the cells were washed 3 times with TRIS-Q, and incubated 15 minutes in this solution. The cells were washed 3 times with PBS-CM and then lysed with PD lysis buffer in the presence of protease inhibitors. Then, the streptavidin-agarose beads previously blocked with milk and washed 3 times with PD buffer were added to the lysates. Finally, beads were pulled-down 1 minute at 6.000 rpm and the supernatant discarded. Pellets were washed 3 times with Wash buffer, dried and resuspended in Sample buffer 2x + DTT. (See Appendix Table 7.5 for biotinylation solutions composition).

4. Results

4.1 Generation of CFP-tagged NIS-HA constructs

The chosen cloning strategy was based on the PCR amplification of the coding sequences of NIS-HA and of NIS cytoplasmic C-terminal domain using PCR primers, in which selected restriction enzyme recognition sites were added to their ends. This allowed to create recognition sites on the PCR fragment and subsequently subclone it to the desired plasmid in a specific position and orientation. This was the first and a very important step, once only after the amplifications were successful, it was possible to start the synthesis of the protein CFP-tagged NIS-HA constructs (Fig. 4.1). PCR products obtained were then digested and ligated into the receptor plasmids to obtain the final constructs. The schematic representations of the protein constructs generated are represented in Fig. 4.2 A and B respectively.

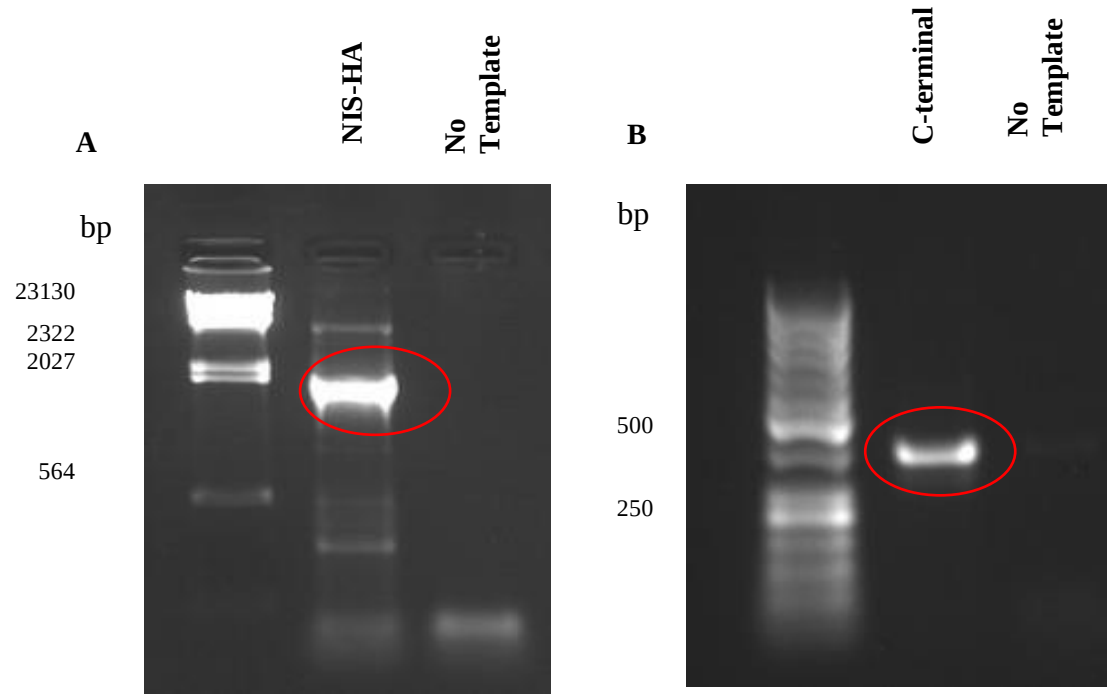

Figure 4.1 – Screening electrophoresis of the amplification of NIS-HA and NIS-HA´s C-terminal coding sequences. (A) NIS-HA coding sequence amplified using 5´Nhe and 3´HindIII; The amplification is observed around the 2000bps. WM: DNA molecular weight marker Lambda DNA/HindIII (B) NIS-HA´s C-terminal coding sequence amplified using 5´BsrG1 and 3´Not 1; The amplification is observed around the 400 bps Both mock controls are cleared. WM: DNA molecular weight marker GeneRuler 50 bp DNA Ladder. No amplification was observed in no template controls.

A

. NIS-HA-CFP

. NIS-HA-CFP-Cter

. NIS-HA-CFP-pre-Cter

B

. NIS-HA-CFP

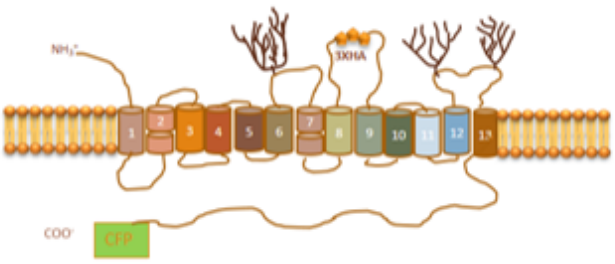

. NIS-HA-CFP-pre-Cter

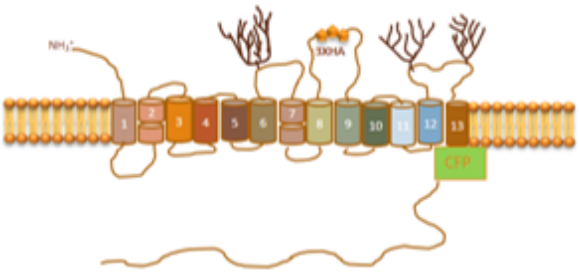

. NIS-HA-CFP-Cter

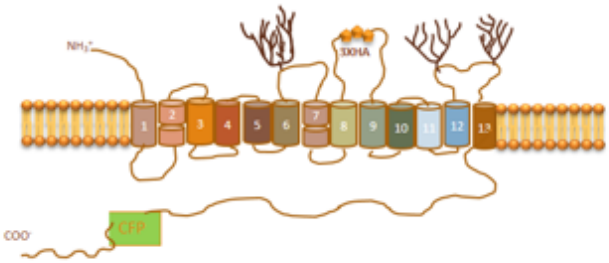

Figure 4.2 – Schematic representations of the CFP-tagged NIS-HA protein constructs. (A) Coding domains (B) Protein structure.

4.2 Levels of expressions of CFP-tagged NIS-HA constructs

The expression levels of the newly developed CFP-tagged NIS-HA constructs were firstly evaluated in HEK293 cells. This cell line was chosen to make a first assessment of constructs' expression since considerably high expression rates can be achieved with transiently transfected HEK293 cells.

Thus, constructs were transiently expressed in this cell line and protein levels were assessed by Western Blot. Due to the presence of both CFP and triple HA protein tags in the newly developed protein constructs, Western blot were performed using both primary anti-HA and anti-CFP antibodies. Although we observed protein expression from all the constructs tested, we found that the expression levels of NIS-HA-CFP-pre-Cter were the lowest of the three (Fig. 4.3). Confirming the specificity of the test, we further observed that NIS-HA (lacking the CFP tag) was only detected using the primary anti-HA antibody and the PeCFP-N1 empty vector (lacking the HA tag) was only detected using the primary anti-CFP antibody. Detection of PCNA antibody was used as loading control (Fig. 4.3).

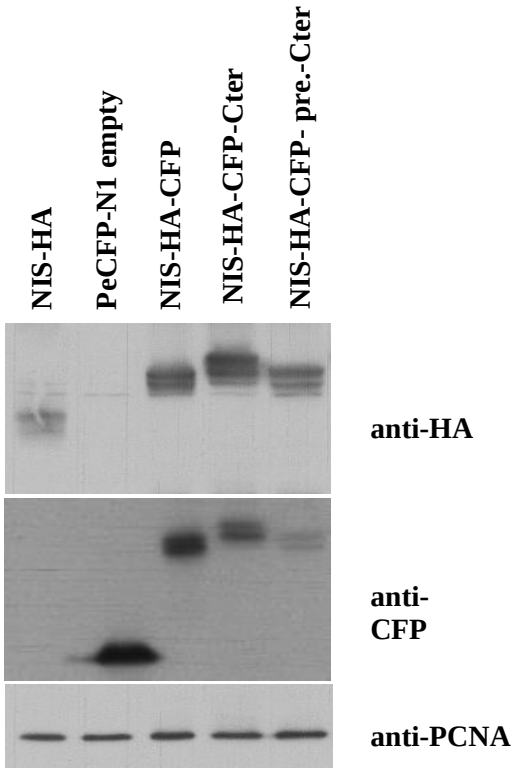

Figure 4.3 – CFP-tagged NIS-HA constructs´ total expression levels in HEK293 cells. Western blot analysis using anti-HA and anti-CFP antibodies in 1:500 and 1:2000 dilution, respectively. NIS-HA-CFP-pre-Cter showed the lowest level of expression of the three constructs. NIS-HA (CFP untagged) showed expression only when using anti-HA antibody.

Then, we addressed whether the differences in total protein expression levels translated into similar differences in terms of the membrane-associated protein fractions. We started by assessing plasma membrane abundance of the newly developed CFP-tagged NIS constructs in transiently transfected HEK293 cells using a cell surface protein biotinylation assay (see methods).

We observed that the tested CFP-tagged NIS constructs were pulled down with the membrane associated protein fraction (PD). The amount of CFP-tagged NIS-HA proteins at the cell surface, however, was lower compared with control NIS-HA (without CFP tag). Among the three constructs tested, NIS-HA-CFP-Cter appears to be that with the highest expression at the plasma membrane, despite showing lower expression levels in comparison with NIS-HA-CFP, when total protein was analyzed. NIS-HA-CFP-pre-Cter, on the other hand, despite having the lowest total protein expression,

considerable levels of protein are still observed in the membrane-associated protein fraction. In addition, neither NIS-HA in the negative control (without biotin) nor PCNA (which has a cytoplasmatic location) were present in relevant levels in the PD fractions, confirming the assay specificity (Fig.4.4).

To address the behaviour of CFP-tagged NIS-HA constructs in a malignant thyroid context the same procedure was followed for TPC-1 cells. Western blot detection of CFP-tagged NIS-HA proteins was performed using anti-HA antibody and non CFP-tagged NIS-HA was used as positive control of cell surface residency. Interestingly, in this cellular system, NIS-HA-CFP-Cter was the one with highest expression in terms of total protein (PT), which also translates into the highest cell surface expression (PD). With regard to NIS-HA-CFP-pre-Cter, based on this assay, its presence at the cell surface was inconclusive, since its level of expression in this cell model seemed to be extremely low, precluding its detection by Western blot even through total protein analysis (PT) (Fig. 4.4).

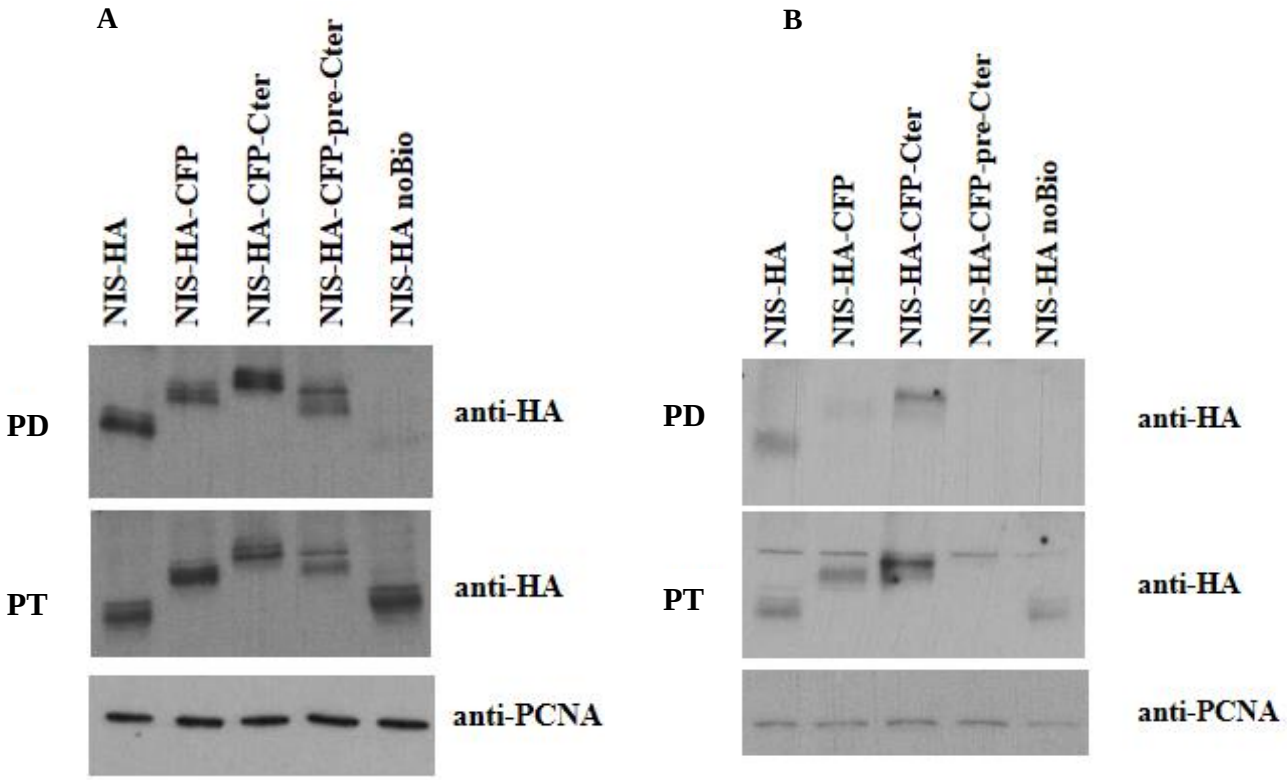

Figure 4.4 – NIS-HA protein constructs´ total (PT) and plasma membrane (PD) expression levels in HEK293 and TPC-1 cells. Western blot analysis using anti-HA at a 1:500. The levels of expression were lower at TPC-1 cells both in total and in plasma membrane, being NIS-HA-CFP-Cter the one with the highest expression (A) NIS-HA protein constructs levels of expression in HEK293 cells; (B) NIS-HA protein constructs levels of expression in TPC-1 cells.

4.3 Fluorescence Microscopy

Next, we addressed the expression and cellular localization of the newly developed CFP-tagged NIS-HA constructs by fluorescence microscopy in HEK293 cells. Labelling of F-actin with phalloidin-TRITC was used to observe cell morphology, particularly, to identify the cell cortex (actomyosin cortex) in the inner face of the cell membrane. Non-CFP-tagged NIS-HA was also included as control for NIS location at the plasma membrane. In this case, given the absence of the fluorescent tag, the detection

was done using an anti-HA primary antibody followed by Alexa Fluor 488-conjugated secondary antibody (Fig. 4.5). As expected from the Western blot analysis, NIS-HA-CFP appeared to be, among the newly developed constructs, the one with the highest expression, followed by NIS-HA-CFP-Cter and then NIS-HA-CFP-pre-Cter. It should be noted that all CFP-tagged constructs showed lower levels of expression than the control without the CFP tag. It is also worth noting that NIS-HA-CFP, despite being the most expressed, seemed to have a distinct cellular distribution compared to the other NIS constructs. In fact, NIS-HA-CFP showed an accumulation in what seems to be the perinuclear region with low staining observed at the cortical region. On the other hand, NIS-HA-CFP-Cter showed to co-localize with phalloidin in define regions at the periphery of the cell. In this case no accumulation at the perinuclear region was observed. Finally, NIS-HA-CFP-pre-Cter staining was not conclusive in terms of perinuclear region accumulation. However, localization at the periphery of the cell was observed (Fig. 4.5). To clarify whether the staining observed at the periphery of the cell could actually result from the presence of CFP-tagged NIS-HA constructs at the plasma membrane, we took advantage of the extracellular location of the HA tag (which was inserted in the 4th extracellular loop of NIS) to confirm its presence at the cell surface. The extracellular HA tag would thus allow the analysis of NIS surface abundance and retention by direct immunofluorescence labelling of membrane-resident NIS-HA (either CFP-tagged or untagged) in intact cells. Briefly, CFP-tagged NIS-HA constructs present at the cell surface were selectively labelled with anti-HA primary antibody (followed by Alexa Fluor 532-conjugated secondary antibody) in non-permeabilized cells (only extracellular HA-tags are recognized by the antibody). Under these experimental conditions, a specific staining was observed at the cell periphery likely resulting from the presence of the CFP-tagged NIS-HA constructs at the cell surface. We also observed that cell-surface stainings of CFP-tagged NIS-HA constructs appeared to be weaker than the observed for NIS-HA (CFP-untagged), particularly in TPC-1 cells. Regarding NIS-HA-CFP, the CFP-tagged construct showing highest expression, a strong staining at the cell surface was observed despite the accumulation in the perinuclear region observed in the previous assessment (Fig 4.6).

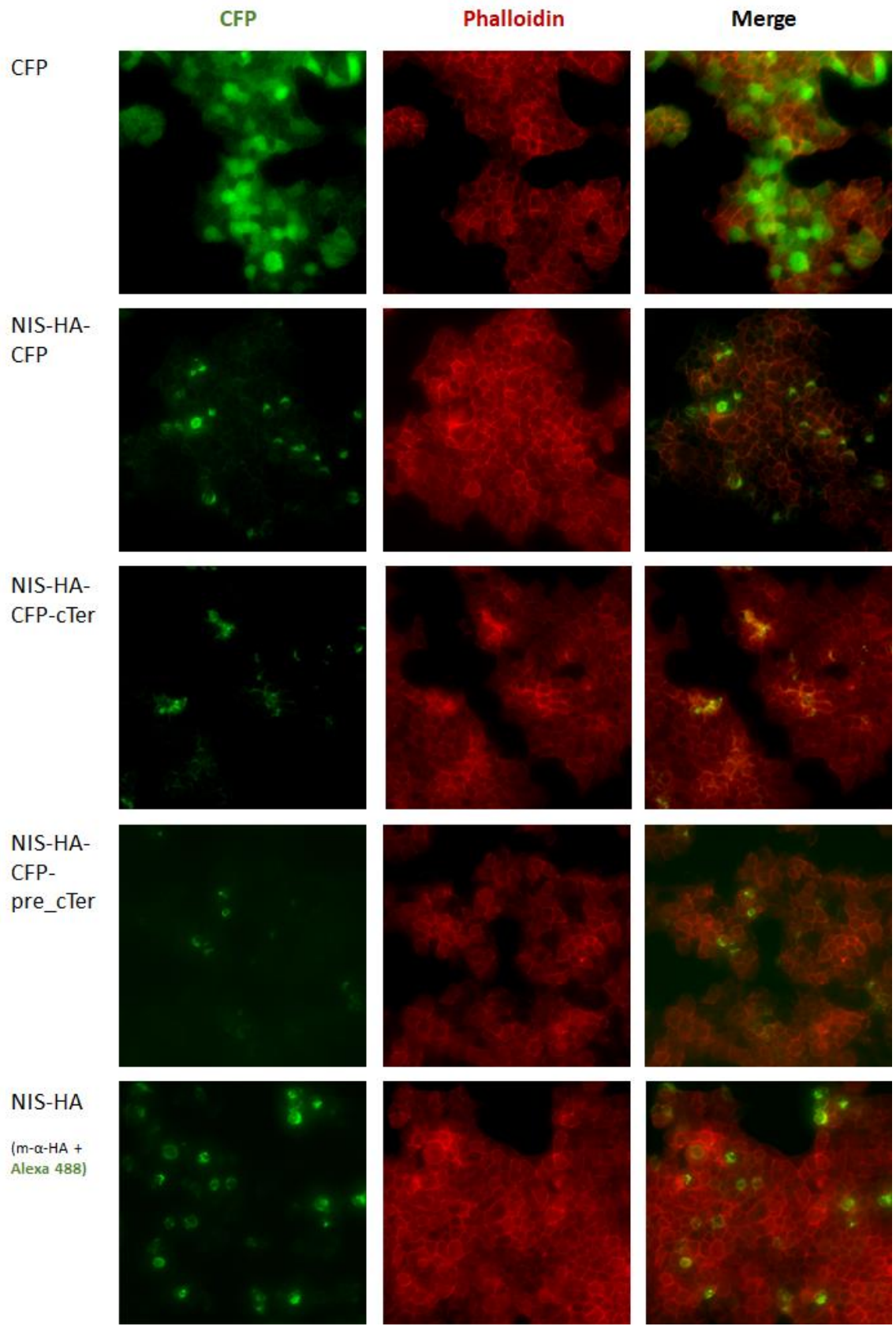

Figure 4.5 – Fluorescence analysis of CFP-tagged NIS-HA constructs in HEK293 cells. CFP-tagged NIS-HA constructs expression and localization was observed using CFP fluorescence. Labelling of F-actin with phalloidin-TRITC was used to show the overall shape and structure of the cell, particularly the cortex in the inner face of the cell membrane. Non-CFP-tagged NIS-HA was included as control of NIS location at the plasma membrane and its detection was done using an anti-HA primary antibody followed by Alexa Fluor 488-conjugated secondary antibody. Total magnification 200x.

Nevertheless, NIS-HA-CFP-Cter, despite having a lower level of expression, also showed a strong staining at the cell surface. In TPC1, in particular, NIS-HA-CFP-Cter processing and trafficking towards the cell surface seemed more effective than NIS-HA-CFP. On the other hand, the NIS-HA-CFP-pre-Cter showed a very weak staining at the cell surface, being almost undetectable in TPC-1 cells (Fig. 4.6).

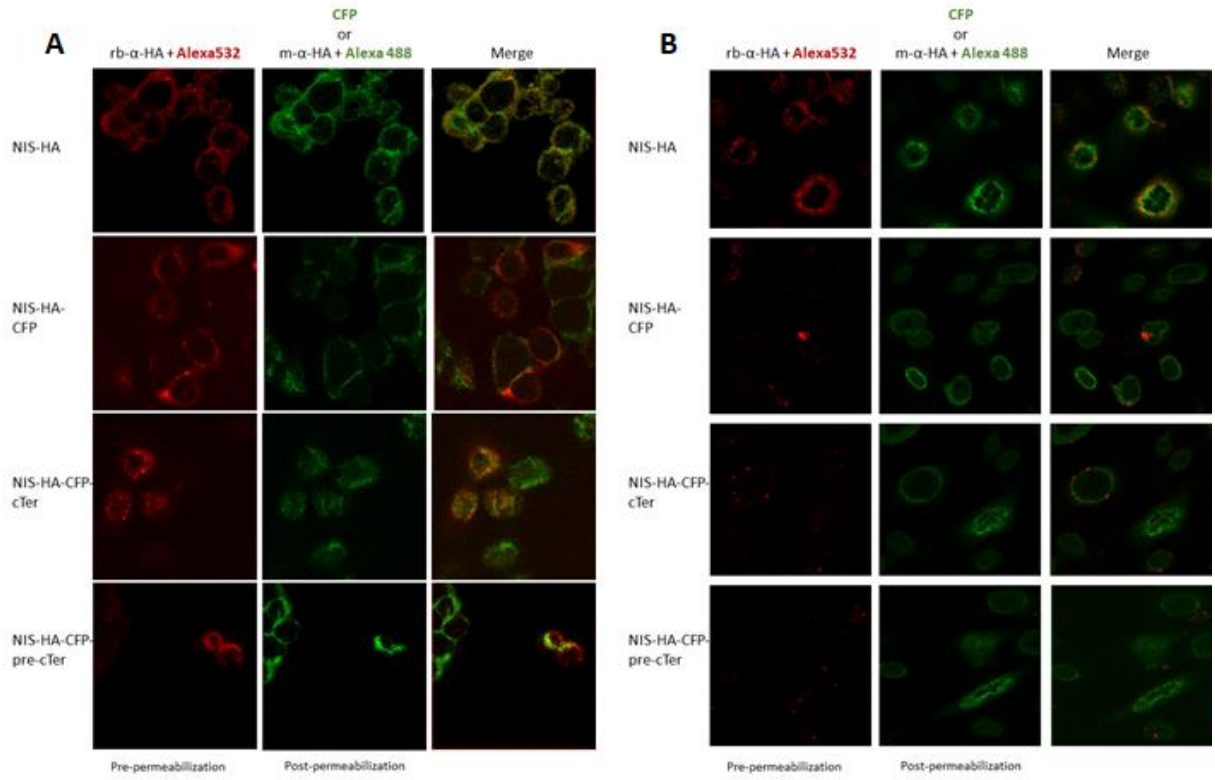

Figure 4.6 – Detection of membrane associated CFP-tagged NIS-HA constructs in (A) HEK293 and (B) TPC-1 cells. The presence of extracellular HA-tag in CFP-tagged NIS-HA constructs allows its selective detection at the plasma membrane of intact cells. Cells expressing NIS-HA constructs, were incubated on ice with rabbit anti-HA to immunolabel only extracellularly HA-tagged NIS proteins at the PM. Cells were then thoroughly washed and fixed. CFP-tagged NIS-HA within the whole cell was detected through CFP labelling. For NIS-HA (without CFP-tag), cells were then permeabilized with 0.5% TX-100, followed by incubation with mouse anti-HA to label NIS within the whole cell. Mouse anti-HA was detected with goat anti-mouse Alexa 488 and rabbit anti-HA detected with goat anti-rabbit Alexa 532. Shown are representative confocal microscopy images of the described immunofluorescence stainings. Total magnification 400x.

5. Discussion

Thyroid cancer is the most common endocrine malignancy in the world (Kondo et al.,2006). The initial therapeutic approach for thyroid carcinoma is surgery, but RAI therapy is also a very common treatment and is used to ablate remaining lesions or metastases after total thyroidectomy (Durante et al., 2006). This therapy depends highly on NIS abundance and expression in the plasma membrane of these thyroid tumors. However, NIS expression is diminished in TC and therefore iodide transport is also low when compared with normal thyroid (Kogai, T. et al.,2006). The abnormalities in NIS transport and delivery to the plasma membrane in TC will reduce the effect of RAI therapy. Therefore, it is very important to understand more about the regulation and mechanisms of NIS trafficking to the plasma membrane in order to improve NIS mediated RAI therapy. The establishment of tagged-NIS cell lines and assessment of its functional integrity, will further allow the functional validation of molecular targets to enhance NIS functional expression and iodide uptake efficiency, increasing the efficacy of radioiodide therapy.

It is physiologically essential for the accumulation of iodide from the bloodstream into thyroid follicular cells that NIS is expressed at the basolateral plasma membrane of the thyroid follicle. In this study, our group developed three CFP-tagged NIS-HA constructs that may allow the specific detection of NIS from its biosynthesis to its delivery and retention at the plasma membrane. These constructs may also be useful for the comparison of NIS processing and membrane trafficking in diverse cellular systems, despite having distinct levels of endogenous NIS expression, since potential interferences resulting from NIS transcriptional regulation will be avoided. We showed that all the newly developed constructs were expressed in the two cell lines tested, being also able to reach the cell surface, which was one of our main goals. However, in HEK293 and TPC-1 cells the abundance at the plasma membrane of the CFP-tagged NIS-HA constructs turned out to be very low, even when total expression was high. Since this was observed in both malignant and non-malignant cell systems, we hypothesized that the low abundance of CFP-tagged NIS constructs in the plasma membrane may be due to failures in post-translational processing, which in turn may be related to the presence of the CFP in the NIS C-terminal domain. In fact, the C-terminal domain of NIS has several phosphorylation sites, ligation sites, as well as other important motifs for NIS sorting and delivery to the plasma membrane (Fanning, A.S. and Anderson, J.M.,1999; Tan, P.K. et al.,1998; Dietrich, J. et al.,1997) and the presence of the CFP tag could somehow interfere with the recognition and proper folding of these key motifs. In fact, in TPC-1 in particular, NIS-HA-CFP-Cter appeared to be the most abundant at the cell surface. In this construct, the C-terminal domain of NIS was duplicated, which might be contributing to the preservation of C-terminal´s regulatory elements and therefore to an enhanced membrane trafficking and retention, in comparison to the other two constructs tested. The possibility that NIS membrane trafficking is subjected to specific regulatory processes is supported by NIS protein being expressed in tissues other than thyroid. Considering different tissue specific iodide requirements, NIS expression in different tissues also displays different membrane expression patterns in polarized cells (e.g basolateral vs apical localization). Therefore, uncharacterized factors, other than the NIS sequence may regulate NIS sorting to the plasma membrane, and these may be affected by the presence of the CFP tag.

While the establishment of the CFP-tagged NIS-HA constructs was successfully accomplished, more studies are needed in order to evaluate their functional expression. In fact, due to the impact of Covid-19 pandemics that resulted in the lock down of FMUL laboratory from March 2020 to June 2020, causing a delay in experimental plan and expected results, we were not able to perform some of the studies and assays previously planned, particularly, the functional validation of the constructs

developed. An extremely relevant assay for this purpose would have been the iodide influx assay, that allows the evaluation of the capacity of the newly synthetize CFP-tagged NIS-HA constructs to uptake iodide into the cells. So, in future studies, this will be evaluated using the YFP-based, non-radioactive, iodide influx assay. The cellular models to be used will be modified to constitutively express the yellow fluorescent protein YFP-H148Q/I152L, a halide sensitive mutant that is quenched by iodide (Y-cells). This fluorescent sensor enables rapid changes in iodide intracellular concentration to be monitored by live cell. The iodide influx will be assayed by recording cell fluorescence after exposure to a high iodide concentration. Iodide influx through NIS will cause the quenching of YFP decreasing cell fluorescence recordings in comparison to initial values, before iodide addition. The assay can be used to monitor either overall influx in a cell population, using microplate readers, or to follow single cell responses by time-lapse microscopy. This will be important to assess dose-dependent effects of candidate targets for therapeutic intervention. Thus, the selected CFP-tagged NIS-HA constructs will be used to establish cell models stably expressing CFP-tagged NIS-HA proteins. These will then be pharmacologically targeted, either directly or through known protein and pathways modulators. This will allow the evaluation of NIS functional expression upon different conditions and identify those able to increase its maturation, trafficking and abundance at the plasma membrane and, ultimately, to be used to enhance the uptake of iodide by TC cells. It will also be interesting to study the impact of RAC1 in NIS trafficking to the plasma membrane. It has been shown that RAC1 has a pivotal role in the regulation of the plasma membrane abundance of several ion channels such as chloride channels (Moniz S. et al 2013) and the epithelium sodium channel (Karpushev AV. et al 2011). Also, previous studies from our group have implicated RAC1 in the enhancement of NIS expression at the transcriptional level. It remains to be determined whether it will also impact NIS trafficking to the plasma membrane

In conclusion we could say that NIS-HA-CFP appeared to be, among the newly developed constructs, the one with the highest expression, followed by NIS-HA-CFP-Cter and then NIS-HA-CFP-pre-Cter. All CFP-tagged constructs showed lower levels of expression than the control without the CFP tag. It is also worth noting that NIS-HA-CFP seemed to have a distinct cellular distribution comparing to the other NIS constructs. NIS-HA-CFP showed an accumulation in what seems to be the perinuclear region while NIS-HA-CFP-Cter showed to be in defined regions at the periphery of the cell. On the other hand, NIS-HA-CFP-pre-Cter staining was not conclusive in term of perinuclear region accumulation, however, localization at the periphery of the cell was observed. In terms of NIS surface abundance and retention, specific staining was observed at the cell periphery likely resulting from the presence of the CFP-tagged NIS-HA constructs at the cell surface. We also observed that cell-surface stainings of CFP-tagged NIS-HA constructs appeared to be weaker to that of NIS-HA (CFP-untagged). NIS-HA-CFP and NIS-HA-CFP-Cter, despite having different levels of expression, showed a strong staining at the cell surface, however, NIS-HA-CFP-Cter processing and trafficking towards the cell surface seems more effective. The NIS-HA-CFP-pre-Cter showed a very weak staining at the cell surface. Despite these results, it remains to be determined which of the constructs should be selected considering their functional expression, since more studies would be needed to reach this conclusion.

6. References

Abbosh, P.H., Nephew, K.P. 2005. Multiple signaling pathways converge on beta-catenin in thyroid cancer. Thyroid. 551–561;

Abubaker, J., Jehan, Z., Bavi, P., Sultana, M., Al-Harbi, S., Ibrahim, M., Al-Nuaim, A. 2008. Clinicopathological analysis of papillary thyroid cancer with PIK3CA alterations in a Middle Eastern population. J Clin Endocrinol Metab. 611–618;

Ahn, B.C. 2011. Applications of molecular imaging in drug discovery and development process. Curr Pharm Biotechnol. 459-68;

Ahn, B.C., Lee, S.W., Lee, J., Kim, C. 2011. Pulmonary aspergilloma mimicking metastasis from papillary thyroid cancer. Thyroid. 555-8;

Ahn, S.J., Jeon, Y.H., Lee, Y.J, Lee, Y.L, Lee, S.W., Ahn, B.C. 2010. Enhanced anti-tumor effects of combined MDR1 RNA interference and human sodium/iodide symporter (NIS) radioiodine gene therapy using an adenoviral system in a colon cancer model. Cancer Gene Ther. 492-500;

Ajjan, R.A., Watson, P.F., Findlay, C., Metcalfe, R.A., Crisp, M., Ludgate, M., Weetman, A.P. 1998. The sodium iodide symporter gene and its regulation by cytokines found in autoimmunity. J Endocrinol 158. 351–358;

Al-Jundi, M., Thakur, S., Gubbi, S., Klubo-Gwiezdzinska, J. 2020. Novel Targeted Therapies for Metastatic Thyroid Cancer—A Comprehensive Review. Cancers 2020 12. 2104;

Bahn Chair, R.S., Burch, H.B., Cooper, D.S., Garber, J.R., Greenlee, M.C., Klein, I. 2011. Hyperthyroidism and other causes of thyrotoxicosis: management guidelines of the American Thyroid Association and American Association of Clinical Endocrinologists. Thyroid. 593-646;

Baril, P., Martin-Duque, P., Vassaux, G. 2010. Visualization of gene expression in the live subject using the Na/I symporter as a reporter gene: applications in biotherapy. Br J Pharmacol. 761-71;

Barton, K.N., Stricker, .H, Brown, S.L., Elshaikh, M., Aref, I., Lu, M. 2008. Phase I study of noninvasive imaging of adenovirus-mediated gene expression in the human prostate. Mol Ther. 1761-9;

Bauerle, K.T., Schweppe, R.E, Haugen, B.R. 2010. Inhibition of nuclear factor-kappa B differentially affects thyroid cancer cell growth, apoptosis, and invasion. Mol Cancer. 117;

Begum, S., Rosenbaum, E., Henrique, R., Cohen, Y., Sidransky, D., Westra, W.H. 2004. BRAF mutations in anaplastic thyroid carcinoma: implications for tumor origin, diagnosis and treatment. Mod. Pathol. 17. 1359–1363;

Bible, K.C., Ryder, M. 2016. Evolving molecularly targeted therapies for advanced-stage thyroid cancers. Nat Rev Clin Oncol. 403-16;

Bid, H. K., Roberts, R.D., Manchanda, P.K., Houghton, P.J. 2013. RAC1: an emerging therapeutic option for targeting cancer angiogenesis and metastasis. Mol Cancer Ther. 12. 1925-34;

Bidart, J.M., Lacroix, L., Evain-Brion, D., Caillou, B., Lazar, V., Frydman, R., Bellet, D., Filetti, S., Schlumberger, M. 2000. Expression of Na^+/I^- symporter and Pendred syndrome genes in trophoblast cells. J. Clin. Endocrinol. Metab., 4367-4372;

Bizhanova, A., Kopp, P. 2009. Minireview: the sodium-iodide symporter NIS and pendrin in iodide homeostasis of the thyroid. Endocrinology 150. 1084–1090;

Boelaert, K., Smith, V. E., Stratford, A. L., Kogai, T., Tannahill, L. A., Watkinson, J. C. 2007. PTTG and PBF repress the human sodium iodide symporter. Oncogene 26. 4344–4356;

Bommarito, A., Richiusa, P., Carissimi, E., Pizzolanti, G., Rodolico, V., Zito, G., Criscimanna, A. 2011. BRAFV600E mutation, TIMP-1 upregulation, and NF-kappaB activation: closing the loop on the papillary thyroid cancer trilogy. Endocr Relat Cancer. 669–685;

Braverman, L.E., Cooper, D. 2012. Werner and Ingbar's the thyroid. Philadelphia, PA: Lippincott Williams and Wilkins;

Bürgi, H. 2010. Iodine excess. Best Pract. Res. Clin. Endocrinol. Metab. 107–15;

Burrows, N., Babur, M., Resch, J., Ridsdale, S., Mejin, M., Rowling, E.J., Brabant, G. 2011. GDC-0941 inhibits metastatic characteristics of thyroid carcinomas by targeting both the phosphoinositide-3 kinase (PI3K) and hypoxia-inducible factor-1alpha (HIF-1alpha) pathways. J Clin Endocrinol Metab. 1934–1943;

Carvalho, D.P., Ferreira, A. 2007. The importance of sodium/iodide symporter (NIS) for thyroid cancer management. Arq Bras Endocrinol Metab. 51;

Castro, M. R., Bergert, E. R., Goellner, J. R., Hay, I. D., Morris, J. C. 2001. Immunohistochemical analysis of sodium iodide symporter expression in metastatic differentiated thyroid cancer: correlation with radioiodine uptake. J Clin Endocrinol Metab 86. 5627–5632;

Cerezo, A., Guadamillas, M. C., Goetz, J. G., Sánchez-Perales, S., Klein, E., Assoian, R. K., Del Pozo, M. A. 2009. The absence of caveolin-1 increases proliferation and anchorage-independent growth by a Racdependent, Erk-independent mechanism. Mol Cell Biol. 29. 5046-59;

Cho, J.Y., Léveillé, R., Kao, R., Rousset, B., Parlow, A.F., William, E., Burak, Jr., Mazzaferri, E.L., Jhiang, S.M. 2000. Hormonal Regulation of Radioiodide Uptake Activity and Na^+/I^- Symporter Expression in Mammary Glands, The Journal of Clinical Endocrinology & Metabolism 85. 2936–2943;

Chun, J. T., Di Dato, V., D'Andrea, B., Zannini, M., Di Lauro, R. 2004. The CRE-like element inside the 5′-upstream region of the rat sodium/iodide symporter gene interacts with diverse classes of b-Zip molecules that regulate transcriptional activities through strong synergy with Pax-8. Mol Endocrinol 18. 2817–2829;

Chung, J.K. 2002. Sodium iodide symporter: its role in nuclear medicine. J Nucl Med. 1188-200;

Cohen, Y., Xing, M., Mambo, E., Guo, Z., Wu, G., Trink, B., Beller, U., Westra, W.H., Ladenson, P.W., Sidransky, D. 2003. BRAF mutation in papillary thyroid carcinoma. J. Natl. Cancer Inst. 95. 625–627;

Cooper, D.S., Doherty, G.M., Haugen, B.R., Kloos, R.T., Lee, S.L., Mandel, S.J. 2009. Revised American Thyroid Association management guidelines for patients with thyroid nodules and differentiated thyroid cancer. Thyroid. 1167-214;

Costamagna P., Furst K., Tully K. 2004 Tuberculosis associated with blocking agents against tumor necrosis factor-alpha. MMWR: morbidity & mortality weekly report 53. 683- 686;

Dai, G., Levy, O., Carrasco, N. 1996. Cloning and characterization of the thyroid iodide transporter. Nature 379. 458–460;

Darrouzet, E., Lindenthal, S., Marcellin, D., Pellequer, J., Pourcher, T. 2014. The sodium/iodide symporter: State of the art of its molecular characterization, Biochimica et Biophysica Acta (BBA) - Biomembranes 1838. 244-253;

De Benoist, B., McLean, E., Andersson, M., Rogers, L. 2008. Iodine deficiency in 2007: global progress since 2003. Food Nutr. Bull. 29. 195–202;

De Carvalho, F.D., Quick, M. 2011. Surprising substrate versatility in SLC5A6: Na^+ coupled I^- transport by the human Na+/multivitamin transporter (hSMVT). J. Biol. Chem. 286. 131–137;

De Felice, M., Di Lauro, R. 2011. Minireview: intrinsic and extrinsic factors in thyroid gland development: an update. Endocrinology. 2948–56;

De La Vieja, A., Dohan, O., Levy, O., Carrasco, N. 2000. Molecular analysis of the sodium/iodide symporter: impact on thyroid and extrathyroid pathophysiology. Physiol. Rev. 80. 1083-1105;

De la Vieja, A., Reed, M.D., Ginter, C.S., Carrasco, N. 2007. Amino acid residues in transmembrane segment IX of the Na^+/I^- symporter play a role in its Na^+ dependence and are critical for transport activity. J. Biol. Chem. 282. 25290-25298;

De La Vieja, A., Ginter, C.S., Carrasco, N. 2004. The Q267E mutation in the sodium/iodide symporter (NIS) causes congenital iodide transport defect (ITD) by decreasing the NIS turnover number. J. Cell Sci. 117. 677-687;

DiDonato, J.A., Mercurio, F., Karin, M. 2012. NF-kappaB and the link between inflammation and cancer. Immunol Rev. 379–400;

Dietrich, J., Kastrup, J., Nielsen, B.L., Odum, N., Geisler, C. 1997. Regulation and function of the CD3 γ DxxxLL motif: a binding site for adaptor protein-1 and adaptor protein-2 in vitro. J Cell Biol 138. 271–281;

Dohan, O., De la Vieja, A., Paroder, V., Riedel, C., Artani, M., Reed, M., Ginter, C.S., Carrasco, N. 2003. The sodium/iodide Symporter (NIS): characterization, regulation, and medical significance.

Endocr Rev. 48-77;

Donghi, R., Longoni, A., Pilotti, S., Michieli, P., Della Porta, G., Pierotti, M.A. 1993. Gene p53 mutations are restricted to poorly differentiated and undifferentiated carcinomas of the thyroid gland. J. Clin. Invest. 91. 1753–1760;

Dremier, S., Pohl, V., Smith, C.P., Roger, P.P., Corbin, J., Doskeland, S.O., Dumont, J.E., Maenhaur, C. 1997. Activation of cyclic AMP-dependent kinase is required but may not be sufficient to mimic cyclic AMP-dependent DNA synthesis and thyroglobulin expression in dog thyroid cells. Mol Cell Biol 17. 6717–6726;

Durante, C., Haddy, N., Baudin, E., Leboulleux, S., Hartl, D., Travagli, J.P. 2006. Long-term outcome of 444patients with distant metastases from papillary and follicular thyroid carcinoma: benefits and limits ofradioiodine therapy. J Clin Endocrinol Metab. 2892–2899;

Eline Van Huizen , Gerald M. McInerney. 2020. Activation of the PI3K-AKT Pathway by Old World Alphaviruses. Cells.9;

Elisei, R., Viola, D., Torregrossa, L., Giannini, R., Romei, C., Ugolini, C., Molinaro, E. 2012. The BRAF(V600E) mutation is an independent, poor prognostic factor for the outcome of patients with low-risk intrathyroid papillary thyroid carcinoma: single-institution results from a large cohort study. J Clin Endocrinol Metab. 4390–4398;

Eng, P.H., Cardona, G.R., Previti, M.C., Chin, W.W., Braverman, L.E. 2011. Regulation of the sodium iodide symporter by iodide in FRTL-5 cells. Eur. J. Endocrinol. 144. 139-144;

Eng, P.H.,Cardona, G.R., Fang, S.L., Previti, M., Alex, S., Carrasco, N., Chin, W.W., Braverman, L.E. 1999. Escape from the acute Wolff–Chaikoff effect is associated with a decrease in thyroid sodium/iodide symporter messenger ribonucleic acid and protein. Endocrinology 140. 3404-3410;

Eskandari, S., Loo, D.D., Dai, G., Levy, O., Wright, E.M., Carrasco, N. 1997. Thyroid Na^+/I^- symporter. Mechanism, stoichiometry, and specificity. J. Biol. Chem. 272. 27230-27238

Espadinha, C., Santos, J.R., Sobrinho, L.G., Bugalho, M.J. 2009. Expression of iodine metabolism genes in humanthyroid tissues: evidence for age and BRAFV600Emutation dependency. Clin Endocrinol (Oxf). 629–635;

Fagin, J.A., Matsuo, K., Karmakar, A., Chen, D.L., Tang, S.H., Koeffler, H.P. 1993. High prevalence of mutations of the p53 gene in poorly differentiated human thyroid carcinomas. J. Clin. Invest. 91. 179–184;

Fagin, J.A., Wells, Jr. 2016. Biologic and Clinical Perspectives on Thyroid Cancer. N Engl J Med 375. 1054-1067;

Faham, S., Watanabe, A., Besserer, G.M., Cascio, D., Specht, A., Hirayama, B.A., Wright, E.M., Abramson, J. 2008. The crystal structure of a sodium galactose transporter reveals mechanistic insights into Na^+/sugar symport. Science 321. 810-814;

Fanning, A.S., Anderson, J.M. 1999. PDZ domains: fundamental building blocks in the organization of protein complexes at the plasma membrane. J Clin Invest 103. 767 –772;

Faria, M., Domingues, R., Paixão, F., Bugalho, M. J., Matos, P., Silva, A. L. 2020. TNFα-mediated activation of NF-κB downregulates sodium-iodide symporter expression in thyroid cells. PLOS ONE, 15;

Fernandez, I.J., Piccin, O., Sciascia, S., Cavicchi, O., Repaci, A., Vicennati, V., Fiorentino, M. 2013. Clinical significance of BRAF mutation in thyroid papillary cancer. Otolaryngol Head Neck Surg. 919–925;

Field, J. B., Larsen, P. R., Yamashita, K., Mashiter, K., & Dekker, A. 1973. Demonstration of iodide transport defect but normal iodide organification in nonfunctioning nodules of human thyroid glands. J Clin Invest 52. 2404–2410;

Fragoso, M.A., Fernandez, V., Forteza, R., Randell, S.H., Salathe, M., Conner, G.E. 2004. Transcellular thiocyanate transport by human airway epithelia. J. Physiol. 561. 183-194;

Fujiwara, H., Tatsumi, K., Tanaka, S., Kimura, M., Nose, O., Amino, N. 2000. A novel V59E missense mutation in the sodium iodide symporter gene in a family with iodide transport defect. Thyroid 10. 471-474;

Furlanetto, T.W., Nguyen, L.Q., Jameson, J.L. 1999. Estradiol increases proliferation and down-regulates the sodium/iodide symporter gene in FRTL-5 cells. Endocrinology 140. 5705–5711;

Fusco, A., Chiappetta, G., Hui, P., Garcia-Rostan, G., Golden, L., Kinder, B.K., Dillon, D.A., Giuliano, A., Cirafici, A.M., Santoro, M., Rosai, J., Tallini, G. 2002. Assessment of RET/PTC oncogene activation and clonality in thyroid nodules with incomplete morphological evidence of papillary carcinoma: a search for the early precursors of papillary cancer. Am. J. Pathol. 160 2157–216;

Garcia-Rostan, G., Zhao, H., Camp, R.L., Pollan, M., Herrero, A., Pardo, J., Wu, R., Carcangiu, M.L., Costa, J., Tallini, G. 2003. RAS Mutations Are Associated with Aggressive Tumor Phenotypes and Poor Prognosis in Thyroid Cancer. J. Clin. Oncol 21. 3226–3235;

Gerard, C., Rigot, V., Penel, C. 1994. Chloride channel blockers inhibit the Na^+/I^- symporter in thyroid follicles in culture. Biochem. Biophys. Res. Commun. 204. 1265-1271;

Glavy, J.S., Wu, S.M., Wang, P.J., Orr, G.A., Wolkoff, A.W. 2000. Down-regulation by extracellular ATP of rat hepatocyte organic anion transport is mediated by serine phosphorylation of oatp1. J Biol Chem 275. 1479–1484;

Gonçalves, V., Matos, P., Jordan, P. 2009. Antagonistic SR proteins regulate alternative splicing of tumorrelated RAC1b downstream of the PI3-kinase and Wnt pathways. Human Molecular Genetics. 18. 3696– 3707;

Guigon, C.J., Zhao, L., Willingham, M.C., Cheng, S.Y. 2009. PTEN deficiency accelerates tumour progression in a mouse model of thyroid cancer. Oncogene. 509–517;

Haugen, B. R., Pacini, F., Reiners, C., Schlumberger, M., Ladenson, P. W., Sherman, S. I. 1999. A comparison of recombinant human thyrotropin and thyroid hormone withdrawal for the detection of thyroid remnant or cancer. J Clin Endocrinol Metab 84. 3877–3885;

He, L., Vasiliou, K., Nebert, D.W. 2009.Analysis and update of the human solute carrier (SLC) gene superfamily. Hum. Genomics 3. 195-206;

Hediger, M.A., Romero, M.F., Peng, J.B., Rolfs, A., Takanaga, H., Bruford, E.A. 2004. The ABCs of solute carriers: physiological, pathological and therapeutic implications of human membrane transport proteins. Pflugers Arch. 465-468;

Hingorani, M., Spitzweg, C., Vassaux, G., Newbold, K., Melcher, A., Pandha, H., Vile, R., Harrington, K. 2010. The biology of the sodium iodide symporter and its potential for targeted gene delivery. Curr. Cancer Drug TargetS 10. 242-267;

Ho, A.L., Grewal, R.K., Leboeuf, R., Sherman, E.J., Pfister, D.G., Deandreis, D., Pentlow, K.S., Zanzonico, P.B., Haque, S., Gavane, S., Ghossein, R.A., Ricarte -Filho, J.C., Dominguez, J.M., Shen, R., Tuttle, R.M., Larson, S.M., Fagin, J.A. 2013. Selumetinib-enhanced radioiodine uptake in advanced thyroid cancer. N. Engl. J. Med. 368. 623-632;

Hsieh, A.C., Truitt, M.L., Ruggero, D. 2011. J Cancer. 329-36;

Jeon, Y.H., Ahn, S.J., Lee, Y.J., Lee, Y.L., Lee, S.W., Park, S.Y. 2011. Human sodium iodide symporter added to multidrug resistance 1 small hairpin RNA in a single gene construct enhances the therapeutic effects of radioiodine in a nude mouse model of multidrug resistant colon cancer. Cancer Biother Radiopharm. 671-9;

Jeong, S.Y., Hwang, M.H., Kim, J.E., Kang, S., Park, J.C., Yoo, J. 2011. Combined Cerenkov luminescence and nuclear imaging of radioiodine in the thyroid gland and thyroid cancer cells expressing sodium iodide symporter: initial feasibility study. Endocr J. 575-83;

Jhiang, S.M., Cho, J.Y., Ryu, K.Y., DeYoung, B.R., Smanik, P.A., McGaughy, V.R., Fischer, A.H., Mazzaferri, E.L. 1998. An immunohistochemical study of Na^+/I^- symporter in human thyroid tissues and salivary gland tissues. Endocrinology 139. 4416-4419;

Jordan, P., Brazão, R., Boavida, M. G., Gespach, C., Chastre, E. 1999. Cloning of a novel human RAC1b splice variant with increased expression in colorectal tumors. Oncogene. 18. 6835-6839;

Jung, H. 2002. The sodium/substrate symporter family: structural and functional features. FEBS Lett. 529. 73-77;

Kambe, F., Nomura, Y., Okamoto, T., Seo, H. 1996. Redox regulation of thyroidtranscription factors, Pax-8 and TTF-1, is involved in their increased DNA-binding activities by thyrotropin in rat thyroid FRTL-5 cells. Mol Endocrinol 10. 801–812;

Kameda, Y., Nishimaki, T., Chisaka, O., Iseki, S., Sucov, H. M. 2007. Expression of the epithelial marker E-cadherin by thyroid C cells and their precursors during murine development. J. Histochem. Cytochem. 55. 1075-1088;

Kaminsky, S.M., Levy, O., Salvador, C., Dai, G., Carrasco, N. 1994. Na^+/I^- symporter activity is present in membrane vesicles from thyrotropin-deprived non-I^--transporting cultured thyroid cells. Proc. Natl. Acad. Sci. U.S.A. 91. 3789–3793;

Kaminsky, S.M., Levy, O., Garry, M.T., Carrasco, N. 1991. Inhibition of the Na^+/I^- symporter by harmaline and 3-amino-1-methyl-5H-pyrido(4,3-b)indole acetate in thyroid cells and membrane vesicles. Eur. J. Biochem. 200. 203-207;

Karpushev, AV., Levchenko, V., Ilatovskaya, D., Pavlov, TS., Staruschenko, A. 2011. Novel role of RAC1/WAVE signaling mechanism in regulation of the epithelial Na+ channel. Hypertension 57 (5). 996–1002.

Kawasaki, H., Springett, G.M., Mochizuki, N., Toki, S., Nakaya, M., Matsuda, M., Housman, D.E., Graybiel, A.M. 1998. A family of cAMP-binding proteins that directly activates Rap1. Science 282. 2275–2279;

Kim, J., Ahn, B.C., Hwang, M.H., Lee, H.W., Jeon, Y.H., Jeong, S.Y. 2011. Combined RNA Interference of Hexokinase II and I-131 human Sodium Iodide Symporter Gene Therapy in Anaplastic Thyroid Carcinoma. J Nucl Med. 1756-63;

Kimura, E.T., Nikiforova, M.N., Zhu, Z., Knauf, J.A., Nikiforov, Y.E., Fagin, J.A. 2003. High prevalence of BRAF mutations in thyroid cancer: genetic evidence for constitutive activation of the RET/PTC–RAS–BRAF signaling pathway in papillary thyroid carcinoma. Cancer Res. 63. 1454–1457;

Kogai, T., Brent, G. A. 2012. The sodium iodide symporter (NIS): Regulation and approaches to targeting for cancer therapeutics. Pharmacology & Therapeutics 135. 355-370;

Kogai, T., Endo, T., Saito, T., Miyazaki, A., Kawaguchi, A., Onaya, T. 1997. Regulation by thyroid-stimulating hormone of sodium/iodide symporter gene expression and protein levels in FRTL-5 cells. Endocrinology 138. 2227-2232;

Kogai, T., Sajid-Crockett, S., Newmarch, L. S., Liu, Y., Brent, G. A. 2008. Phosphoinositide-3-kinase inhibition induces sodium/iodide symporter expression in rat thyroid cells and human papillary thyroid cancer cells. Journal of Endocrinology. 199. 243–252;

Kogai, T., Taki, K., & Brent, G. A. 2006. Enhancement of sodium/iodide symporter expression in thyroid and breast cancer. Endocr Relat Cancer 13. 797–826;

Komorowski, J., Pasieka, Z., Jankiewicz-Wika, J., Stepien, H. 2002. Matrix metalloproteinases, tissue inhibitors of matrix metalloproteinases and angiogenic cytokines in peripheral blood of patients with thyroid cancer. Thyroid.655–662;

Kondo, T., Ezzat, S., Asa, S. L. 2006. Pathogenetic mechanisms in thyroid follicular-cell neoplasia. Nat. Rev. Cancer 6. 292–306;

Kosugi, S., Bhayana, S., Dean, H.J. 1999. A novel mutation in the sodium/iodide symporter gene in the largest family with iodide transport defect. J. Clin. Endocrinol. Metab. 84. 3248-3253;

Kosugi, S., Okamoto, H., Tamada, A., Sanchez-Franco, F. 2002. A novel peculiar mutation in the sodium/iodide symporter gene in Spanish siblings with iodide transport defect. J. Clin. Endocrinol. Metab. 87. 3830-3836;

Kosugi, S., Inoue, S., Matsuda, A., Jhiang, S.M. 1998. Novel, missense and loss-of-function mutations in the sodium/iodide symporter gene causing iodide transport defect in three Japanese patients. J. Clin. Endocrinol. Metab. 83. 3373-3376;

Kotani, T., Ogata, Y., Yamamoto, I., Aratake, Y., Kawano, J.I., Suganuma, T., Ohtaki, S. 1998. Characterization of gastric Na^+/I^- symporter of the rat. Clin. Immunol. Immunopathol. 89. 271-278;

Kroll, T.G., Sarraf, P., Pecciarini, L., Chen, C.J., Mueller, E., Spiegelman, B.M., Fletcher, J.A. 2000. PAX8-PPARgamma1 fusion oncogene in human thyroid carcinoma. Science 289. 1357–1360;

La Perle, K.M., Kim, D.C., Hall, N.C., Bobbey, A., Shen, D.H., Nagy, R., Wakely Jr., P.E., Lehman, A., Jarjoura, D., Jhiang, S.M. 2013. Modulation of sodium/iodide symporter expression in the salivary gland. Thyroid;

Ladenson, P. W., Braverman, L. E., Mazzaferri, E. L., Brucker-Davis, F., Cooper, D. S., Garber, J. R. 1997. Comparison of administration of recombinant human thyrotropin with withdrawal of thyroid hormone for radioactive iodine scanning in patients with thyroid carcinoma. N Engl J Med 337, 888–896;

Lakshmanan, A., Scarberry, D., Shen, D.H., Jhiang, S.M. 2014. Modulation of sodium iodide symporter in thyroidcancer. Horm Cancer. 363–373;

Lazar, V., Bidart, J.M., Caillou, B., Mahe´C, Lacroix, L., Filetti, S. 1999. Expression of the Na+/I-symportergene in human thyroid tumors: a comparison study with other thyroid-specific genes. J Clin EndocrinolMetab. 3228–3234;

Lecat-Guillet, N., Ambroise, Y. 2008. Discovery of aryltrifluoroborates as potent sodium/iodide symporter (NIS) inhibitors. ChemMedChem 3. 1207-1209;

Lee, Y.L., Lee, Y.J., Ahn, S.J., Choi, T.H., Moon, B.S., Cheon, G.J. 2010. Combined radionuclide-chemotherapy and in vivo imaging of hepatocellular carcinoma cells after transfection of a triple-gene construct, NIS, HSV1-sr39tk, and EGFP. Cancer Lett. 129-38;

Leonardi, G.C., Candido, S., Carbone, M., Raiti, F., Colaianni, V., Garozzo, S., Cina, D. 2012. BRAF mutations in papillary thyroid carcinoma and emerging targeted therapies (review) Mol Med Rep. 687–694;

Levy, O., De la Vieja, A., Ginter, C.S., Riedel, C., Dai, G., Carrasco, N. 1998. N-linked glycosylation of the thyroid Na^+/I^- symporter (NIS). Implications for its secondary structure model. J. Biol. Chem. 273. 22657-22663;

Levy, O., Ginter, C.S., De la Vieja, A., Levy, D., Carrasco, N. 1998. Identification of a structural requirement for thyroid Na^+/I^- symporter (NIS) function from analysis of a mutation that causes human congenital hypothyroidism. FEBS Lett. 429. 36-40;

Li, C., Lee, K.C., Schneider, E.B., Zeiger, M.A. 2012. BRAF V600E mutation and its association with clinicopathological features of papillary thyroid cancer: a meta-analysis. J Clin Endocrinol Metab. 4559–4570;

Li, X., Abdel-Mageed, A.B., Mondal, D., Kandil, E. 2013. The nuclear factor kappa-B signaling pathway as a therapeutic target against thyroid cancers. Thyroid. 209–218;

Liang, J.A., Chen, C.P., Huang, S.J., Ho, T.Y., Hsiang, C.Y., Ding, H.J., Wu, S.L., 2005. A novel loss-of-function deletion in sodium/iodide symporter gene in follicular thyroid adenoma. Cancer Lett. 230. 65-71;

Lim, J.Y., Hong, S.W., Lee, Y.S., Kim, B.W., Park, C.S., Chang, H.S., Cho, J.Y. 2013. Clinicopathologic implications of the BRAF(V600E) mutation in papillary thyroid cancer: a subgroup analysis of 3130 cases in a single center. Thyroid. 1423–1430;

Liu, B., Kuang, A. 2012. Genetic alterations in MAPK and PI3K/Akt signaling pathways and the generation, progression, diagnosis and therapy of thyroid cancer. Sheng Wu Yi Xue Gong Cheng Xue Za Zhi. 1221–1225;

Liu, D., Hu, S., Hou, P., Jiang, D., Condouris, S., Xing, M. 2007. Suppression of BRAF/MEK/MAP kinase pathway restores expression of iodide-metabolizing genes in thyroid cells expressing the V600E BRAF mutant. Clinical Cancer Research. 13. 1341–1349;

Liu, J., Brown, R.E. 2012. Morphoproteomic confirmation of an activated nuclear factor-small ka, CyrillicBp65 pathway in follicular thyroid carcinoma. Int J Clin Exp Pathol. 216–223;

Liu, Z., Hou, P., Ji, M., Guan, H., Studeman, K., Jensen, K., Vasko, V. 2008 Highly prevalent genetic alterations in receptor tyrosine kinases and phosphatidylinositol 3-kinase/akt and mitogen-activated protein kinase pathways in anaplastic and follicular thyroid cancers. J Clin Endocrinol Metab. 3106–3116;

Loo, D.D., Hirayama, B.A., Meinild, A.K., Chandy, G., Zeuthen, T., Wright, E.M. 1999. Passive water and ion transport by cotransporters. J. Physiol. 518. 195-202;

Manie, S., Santoro, M., Fusco, A., Billaud, M. 2001. The RET receptor: function in development and dysfunction in congenital malformation. Trends Genet. 17. 580–589;

Mansouri, A., Chowdhury, K., Gruss, P. 1998. Follicular cells of the thyroid gland require Pax8 gene function. Nat Genet 19 87–90;

Marks, M.S., Ohno, H., Kirchhausen, T., Bonifacino, J.S. 1997. Protein sorting by tyrosine-based signals: adapting to the Ys and wherefores. Trends Cell Biol 7. 124–128;

Matos, P., Collard, J. G., Jordan, P. 2003. Tumor-related Alternatively Spliced RAC1b Is Not Regulated by Rho-GDP Dissociation Inhibitors and Exhibits Selective Downstream Signaling. The Journal of Biological Chemistry. 278. 50442–50448;

Matos, P., Skaug, J., Marques, B., Beck, S., Veríssimo, F., Gespach. C., Boavida, M.G., Scherer, S.W. & Jordan, P. 2000. Small GTPase RAC1: structure, localization, and expression of the human gene. Biochemical and Biophysical Research Communications. 277. 741–751;

Matsuda, A., Kosugi, S. 1997. A homozygous missense mutation of the sodium/iodide symporter gene causing iodide transport defect J. Clin. Endocrinol. Metab. 82. 3966-3971;

Maxon, H. R., Smith, H. S. 1990. Radioiodine-131 in the diagnosis and treatment of metastatic well differentiated thyroid cancer. Endocrinol Metab Clin North Am 19. 685–718;

Mizukami, Y., Hashimoto, T., Nonomura, A., Michigishi, T., Nakamura, S., Noguchi, M. 1994. Immunohistochemical demonstration of thyrotropin (TSH)-receptor in normal and diseased human thyroid tissues using monoclonal antibody against recombinant human TSH-receptor protein. J Clin Endocrinol Metab 79. 616–619;

Moniz, S., Sousa, M., Moraes, BJ., Mendes, AI., Palma, M., Barreto, C., Fragata, JI., Amaral, MD., Matos, P. 2013. HGF stimulation of RAC1 signaling enhances pharmacological correction of the most prevalent cystic fibrosis mutant F508del-CFTR. ACS chemical biology 8(2). 432–442.

Montanelli, L., Agretti, P., Marco, G., Bagattini, B., Ceccarelli, C., Brozzi, F., Lettiero, T., Cerbone, M., Vitti, P., Salerno, M., Pinchera, A., Tonacchera, M. 2009. Congenital hypothyroidism and late-onset goiter: identification and characterization of a novel mutation in the sodium/iodide symporter of the proband and family members. Thyroid 19. 1419-1425;

Moshfegh, Y., Bravo-Cordero, J.J., Miskolci, V., Condeelis, J., Hodgson, L. A. 2014. Trio-RAC1-Pak1 signalling axis drives invadopodia disassembly. Nat Cell Biol. 16. 574-86;

Nicola, J.P., Basquin, C., Portulano, C., Reyna-Neyra, A., Paroder, M., Carrasco, N. 2009. The Na^+/I^- symporter mediates active iodide uptake in the intestine. Am. J. Physiol. Cell Physiol.296. 654-662;

Nikiforova, M.N., Caudill, C.M., Biddinger, P., Nikiforov, Y.E. 2002. Prevalence of RET/PTC rearrangements in Hashimoto's thyroiditis and papillary thyroid carcinomas. Int. J. Surg. Pathol. 10. 15–22;

Nikiforova, M.N., Lynch, R.A., Biddinger, P.W., Alexander, E.K., Dorn II, G.W., Tallini, G., Kroll, T.G., Nikiforov, Y.E. 2003. RAS point mutations and PAX8-PPAR gamma rearrangement in thyroid tumors: evidence for distinct molecular pathways in thyroid follicular carcinoma. J. Clin. Endocrinol. Metab. 88. 2318–2326;

Nilsson, M., Fagman, H. 2017. Development of the thyroid gland. Development 144. 2123-2140;

Oh, S.W., Moon, S.H., Park, J., Cho, B.Y., Jung, K.C., Lee, D.S. 2011. Combined therapy with (131) I and retinoic acid in Korean patients with radioiodine-refractory papillary thyroid cancer. Eur J Nucl Med Mol Imaging. Eur J Nucl Med Mol Imaging 38. 1798-805;

Ohno, M., Zannini, M., Levy, O., Carrasco, N., Di Lauro, R. 1999. The paired-domain transcription factor Pax8 binds to the upstream enhancer of the rat sodium/iodide symporter gene and participates in both thyroid-specific and cyclic-AMP-dependent transcription. Mol Cell Biol 19. 2051–2060;

Ohta, K., Endo, T., & Onaya, T. 1991. The mRNA levels of thyrotropin receptor, thyroglobulin and thyroid peroxidase in neoplastic human thyroid tissues. Biochem Biophys Res Commun 174. 1148–1153;

Orlichenko, L., Geyer R., Yanagisawa, M., Khauv, D., Radisky, E.S., Anastasiadis, P.Z. 2010. The 19-amino acid insertion in the tumor-associated splice isoform RAC1b confers specific binding to p120 catenin. J Biol Chem. 285. 19153–61;

Pacifico, F., Leonardi, A. 2010. Role of NF-kappaB in thyroid cancer. Mol Cell Endocrinol. 29–35;

Paire, A., Bernier-Valentin, F., Selmi-Ruby, S., Rousset, B. 1997. Characterization of the rat thyroid iodide transporter using anti-peptide antibodies. Relationship between its expression and activity. J. Biol. Chem. 272. 18245-18249;

Palona, I., Namba, H., Mitsutake, N., Starenki, D., Podtcheko, A., Sedliarou, I., Ohtsuru, A. 2006. BRAFV600E promotes invasiveness of thyroid cancer cells through nuclear factor kappaB activation. Endocrinology. 5699–5707;

Pang, X. P., Park, M., Hershman, J. M. 1992. Transforming growth factor-beta blocks protein kinase-A-mediated iodide transport and protein kinase-C-mediated DNA synthesis in FRTL-5 rat thyroid cells. Endocrinology 131. 45–50;

Paroder-Belenitsky, M., Maestas, M.J., Dohan, O., Nicola, J.P., Reyna-Neyra, A., Follenzi, A., Dadachova, E., Eskandari, S., Amzel, L.M., Carrasco, N. 2011. Mechanism of anion selectivity and stoichiometry of the Na^+/I^- symporter (NIS). Proc. Natl. Acad. Sci. U. S. A. 108. 17933-17938;

Perron,B., Rodriguez, A.M., Leblanc, G., Pourcher, T. 2001. Cloning of the mouse sodium iodide symporter and its expression in the mammary gland and other tissues. Journal of Endocrinology 170. 185–196;

Pichler, B.J., Wehrl, H.F., Judenhofer, M.S. 2008. Latest advances in molecular imaging instrumentation. J Nucl Med. 5-23;

Piguet, V., Gu, F., Foti, M., Demaurex, N., Gruenberg, J., Carpentier, J.L., Trono, D. 1999. Nef-induced CD4 degradation: a diacidic-based motif in Nef functions as a lysosomal targeting signal through the binding of β-COP in endosomes. Cell 97. 63–73;

Piper, R.C., Dikic, I., Lukacs, G.L. 2014. Ubiquitin-Dependent Sorting in Endocytosis. Cold Spring Harbor Laboratory Press;

Pisarev, M. A., Thomasz, L., Juvenal, G. J. 2009. Role of transforming growth factor beta in the regulation of thyroid function and growth. Thyroid 19. 881–892;

Pohlenz, J., Medeiros-Neto, G., Gross, J.L., Silveiro, S.P., Knobel, M., S. Refetoff, S. 1997. Hypothyroidism in a Brazilian kindred due to iodide trapping defect caused by a homozygous mutation in the sodium/iodide symporter gene. Biochem. Biophys. Res. Commun. 240. 488-491;

Pohlenz, J., Rosenthal, I.M., Weiss, R.E., Jhiang, S.M., Burant, C., Refetoff, S. 1998. Congenital hypothyroidism due to mutations in the sodium/iodide symporter. Identification of a nonsense mutation producing a downstream cryptic 3′ splice site. J. Clin. Invest. 101. 1028-1035;

Poole, V.L. and McCabe, C.J. 2015. Iodide transport and breast cancer. Journal of Endocrinology 227, 1–12;

Reed-Tsur, M.D., De la Vieja, A., Ginter, C.S., Carrasco, N. 2008. Molecular characterization of V59E NIS, a Na^+/I^- symporter mutant that causes congenital I^- transport defect. Endocrinology 149. 3077-3084;

Reizer, J., Reizer, A., Saier Jr., M.H. 1994. A functional superfamily of sodium/solute symporters. Biochim. Biophys. Acta 1197. 133-166;

Ridley, A. J. 2001. Rho family proteins: coordinating cell responses. Trends In Cell Biol. 11. 471-7;

Ridley, A. J., Schwartz, M. A., Burridge, K., Firtel, R. A., Ginsberg, M. H., Borisy, G., Parsons, J. T. Horwitz, A. R. 2003. Cell migration: integrating signals from front to back. Science. 302. 1704-9;

Riedel, C., De la Vieja, A., Ginter, C.S., Levy, O., Carrasco, N. 1999. TSH regulation of the thyroid iodide transporter (NIS). 2nd American Association of Pharmaceutical Scientists Frontier Symposium: Membrane Transporters and Drug Therapy, Bethesda, MD;

Read, M.L., Seed, R.I., Fong, J.C.W., Modasia, B., Ryan, G.A., Watkins, R.J., Gagliano, T., Smith, V.E., Stratford, A.L., Kwan, P.K., Sharma, N., Dixon, O.M., Watkinson, J.C., Boelaert, K., Franklyn, J.A., Turnell, A.S., McCabe, C.J. 2014. The PTTG1-Binding Factor (PBF/PTTG1IP) Regulates p53 Activity in Thyroid Cells. Endocrinology 155. 1222–1234;

Riedel, C., Levy, O., Carrasco, N. 2001. Post-transcriptional regulation of the sodium/iodide symporter (NIS) by thyrotropin. J. Biol. Chem. 276. 21458-21463;

Riesco-Eizaguirre, G., Leoni, S. G., Mediola, M., Extevez-Cebrero, M. A., Gallego, M. I., Redondo, A., Hardisson, D., Santisteban, P., Vieja, A. 2014. NIS Mediates Iodide Uptake in the Female Reproductive Tract and Is a Poor Prognostic Factor in Ovarian Cancer. Clin Endocrinol Metab.99. 1199–1208 ;

Riesco-Eizaguirre, G., Santisteban, P. 2006. A perspective view of sodium iodide symporter research and its clinical implications. Eur. J. Endocrinol. 155.495-512;

Roman, S., Mehta, P., Sosa, J.A. 2009. Medullary thyroid cancer: early detection and novel treatments. Curr. Opin. Oncol. 21. 5–10;

Rosai, J., Carcangiu, M.L., DeLellis, R.A. 1992. Atlas of Tumor Pathology—Tumors of the Thyroid Gland. 3rd series. Armed Force Institute of Pathology, Washington;

Ross, D.S., Daniels, G.H., Gouveia, D. 1990. The use and limitations of a chemiluminescent thyrotropin assay as a single thyroid function test in an out-patient endocrine clinic. J Clin Endocrinol Metab. 764–9;

Rothenberg, S.M., Daniels, G.H., Wirth, L.J. 2015. Redifferentiation of iodine-refractory BRAF V600E-mutant metastatic papillary thyroid cancer with dabrafenib-response. Clin Cancer Res. 5640–1;

Rousset, B., Dupuy, C., Miot, F., Dumont, J. 2015. Thyroid hormone synthesis and secretion. In Endotext. South Dartmouth, MA, USA;

Russo, D., Damante, G., Puxeddu, E., Durante, C., Filetti, S. 2011. Epigenetics of thyroid cancer and novel therapeutic targets. J. Mol. Endocrinol. 46. 73-81;

Russo, D., Scipioni, A., Durante, C., Ferretti, E., Gandini, L., Maggisano, V., Paoli, D., Verrienti, A., Costante, G., Lenzi, A., Filetti, S. 2011. Expression and localization of the sodium/iodide symporter (NIS) in testicular cells. Endocrine 40. 35-40;

Saez, C., Martinez-Brocca, M. A., Castilla, C., Soto, A., Navarro, E., Tortolero, M. 2006. Prognostic significance of human pituitary tumor-transforming gene immunohistochemical expression in differentiated thyroid cancer. J Clin Endocrinol Metab 91. 1404–1409;

Sale, E.M., Hodgkinson, C.P., Jones, N.P., Sale, G.J. 2006. A new strategy for studying protein kinase B and its three isoforms. Role of protein kinase B in phosphorylating glycogen synthase kinase-3, tuberin, WNK1, and ATP citrate lyase. Biochemistry. 213–223;

Scanlon, K.J. 2004. Cancer gene therapy: challenges and opportunities. Anticancer Res. 501-4
Seo, J.H., Jeon, Y.H., Lee, Y.J., Yoon, G.S., Won, D.I., Ha, J.H. 2010. Trafficking macrophage migration using reporter gene imaging with human sodium iodide symporter in animal models of inflammation. J Nucl Med. 1637-43;

Silva, A. L., Carmo, F., Bugalho M. J. 2013. RAC1b overexpression in papillary thyroid carcinoma: a role to unravel. European Journal of Endocrinology. 168. 795-804;

Sitte, H.H., Farhan, H., Javitch,J.A. 2004. Sodium-dependent neurotransmitter transporters: oligomerization as a determinant of transporter function and trafficking. Mol. Interv. 4. 38-47;

Smith, V.E., Sharma, N., Watkins, R.J., Read, M.L., Ryan, G.A., Kwan, P.P., Martin, A., Watkinson, J.C., Boelaert, K., Franklyn, J.A., McCabe, C.J. 2013. Manipulation of PBF/PTTG1IP Phosphorylation Status; a Potential New Therapeutic Strategy for Improving Radioiodine Uptake in Thyroid and Other Tumors. The Journal of Clinical Endocrinology & Metabolism 98. 2876–2886;

Soares, P., Trovisco, V., Rocha, A.S., Lima, J., Castro, P., Preto, A., Maximo, V., Botelho, T., Seruca, R., Sobrinho-Simoes, M. 2003. BRAF mutations and RET/PTC rearrangements are alternative events in the etiopathogenesis of PTC. Oncogene 22. 4578–4580;

Spitzweg, C., Bible, K.C., Hofbauer, L.C., Morris, J.C. 2014. Advanced radioiodine-refractory differentiated thyroid cancer: the sodium iodide symporter and other emerging therapeutic targets.

Lancet Diabetes Endocrinol. 830–42;

Spitzweg, C., Joba, W., Morris, J.C., Heufelder, A.E. 1999. Regulation of sodium iodide symporter gene expression in FRTL-5 rat thyroid cells. Thyroid 9. 821–830;

Stathatos, N. 2019. Anatomy and Physiology of the Thyroid Gland. In: Luster, M., Duntas, L., Wartofsky, L. (eds) The Thyroid and Its Diseases. Springer;

Stratford, A. L., Boelaert, K., Tannahill, L. A., Kim, D. S., Warfield, A., Eggo, M. C. 2005. Pituitary tumor transforming gene binding factor: a novel transforming gene in thyroid tumorigenesis. J Clin Endocrinol Metab 90. 4341–4349;

Symons, M. 1996. Rho family GTPases: the cytoskeleton and beyond. Trends Biochem Sci. 21. 178–181;

Szinnai, G., Kosugi, S., Derrien, C., Lucidarme, N., David, V., Czernichow, P., Polak, M. 2006. Extending the clinical heterogeneity of iodide transport defect (ITD): a novel mutation R124H of the sodium/iodide symporter gene and review of genotype–phenotype correlations in ITD. J. Clin. Endocrinol. Metab. 91. 1199-1204;

Taki, K., Kogai, T., Kanamoto, Y., Hershman, J. M., Brent, G. A. 2002. A thyroid-specific far-upstream enhancer in the human sodium/iodide symporter gene requires Pax-8 binding and cyclic adenosine 3′,5′-monophosphate response element-like sequence binding proteins for full activity and is differentially regulated in normal and thyroid cancer cells. Mol Endocrinol 16. 2266–2282;

Tan, P.K., Waites, C., Liu, Y., Krantz, D.E., Edwards, R.H. 1998 A leucine-based motif mediates the endocytosis of vesicular monoamine and acetylcholine transporters. J Biol Chem 273. 17351–17360;

Tazebay, H.U., Wapnir, I., Levy, O. 2000. The mammary gland iodide transporter is expressed during lactation and in breast cancer. Nat Med 6. 871–878;

Tell, G., Pellizzari, L., Cimarosti, D., Pucillo, C., Damante, G. 1998. Ref-1 controls pax-8 DNA-binding activity. Biochem Biophys Res Commun 252. 178–183.;

Tonacchera, M., Agretti, P., de Marco, G., Elisei, R., Perri, A., Ambrogini, E., De Servi, M., Ceccarelli, C., Viacava, P., Refetoff, S., Panunzi, C., Bitti, M.L., Vitti, P., Chiovato, L., Pinchera, A. 2003. Congenital hypothyroidism due to a new deletion in the sodium/iodide symporter protein. Clin. Endocrinol. 59. 500-506;

Vadysirisack, D.D., Chen, E.S., Zhang, Z., Tsai, M.D., Chang, G.D., Jhiang,S.M. 2007. Identification of in vivo phosphorylation sites and their functional significance in the sodium iodide symporter. J. Biol. Chem. 282. 36820-36828;

Valenta, L. 1966. Metastatic thyroid carcinoma in man concentrating iodine without organification. J Clin Endocrinol Metab 26. 1317–1324;

Van Sande, J., Massart, C., Beauwens, R., Schoutens, A., Costagliola, S., Dumont, J.E., Wolff, J. 2003. Anion selectivity by the sodium iodide symporter. Endocrinology 144. 247-252;

Veenhoff, L.M., Heuberger, E.H., Poolman, B. 2002. Quaternary structure and function of transport proteins. Trends Biochem. Sci. 27. 242-249;

Vega, F. M., Ridley, A. J. 2008. Rho GTPases in cancer biology. FEBS Lett. 582. 2093-101;

Verburg, F.A., Brans, B., Mottaghy, F. 2011 Molecular nuclear therapies for thyroid carcinoma. Methods;

Vidal, A.P., Andrade, B.M., Vaisman, F., Cazarin, J., Pinto, L.F., Breitenbach, M.M., Corbo, R. 2013. AMP-activated protein kinase signaling is upregulated in papillary thyroid cancer. Eur J Endocrinol. 521–528;

Visciano, C., Prevete, N., Liotti, F., Marone, G. 2015. Tumor-associatedmast cells in thyroid cancer. Int. J. Endocrinol. 705169;

Voorhees, P., Deignan, E., Van Donselaar, E., Humphrey, J., Marks, M.S., Peters, P.J., Bonifacino, J.S. 1995. An acidic sequence within the cytoplasmic domain of furin functions as a determinant of trans-Golgi network localization and internalization from the cell surface. EMBO J 14. 4961–4975;

Vroye, L., Beauwens, R., Van Sande, J., Daloze, D., Braekman, J.C., Golstein, P.E. 1998. The Na^+-I^- cotransporter of the thyroid: characterisation of new inhibitors. Pflugers Arch. 435. 259-266;

Wapnir, I.L., van de Rijn, M., Nowels, K., Amenta, P., Walton, K., Montgomery, K., Greco, R., Dohan, O., Carrasco, N. 2003. Immunohistochemical Profile of the Sodium/Iodide Symporter in Thyroid, Breast, and Other Carcinomas Using High Density Tissue Microarrays and Conventional Sections, The Journal of Clinical Endocrinology & Metabolism 88 1880–1888;

Ward, L. S., Santarosa, P. L., Granja, F., da Assumpcao, L. V., Savoldi, M., Goldman, G. H. 2003. Low expression of sodium iodide symporter identifies aggressive thyroid tumors. Cancer Lett 200. 85–91;

Wolff, J., Chaikoff, I.L. 1948. Plasma inorganic iodide as a homeostatic regulator of thyroid function. J Biol Chem. 555–64;

Wolff, J., Robbins, J., & Rall, J. E. 1959. Iodide trapping without organification in a transplantable rat thyroid tumor. Endocrinology 64.1–11;

Wong, K.K., Zarzhevsky, N., Cahill, J.M., Frey, K.A., Avram, A.M. 2009. Hybrid SPECT-CT and PET-CT imaging of differentiated thyroid carcinoma. Br J Radiol.860-76;

Wright, E.M. 2013. Glucose transport families SLC5 and SLC50. Mol. Aspects Med. 34. 183-196;

Wright, E.M., Loo, D.D., Hirayama, B.A., Turk, E. 2004. Surprising versatility of Na^+–glucose cotransporters: SLC5. Physiology (Bethesda) 19. 370-376;
Wright, E.M., Turk, E. 2004. The sodium/glucose cotransport family SLC5. Pflugers Arch. 447. 510-

518;

Wu, S.L., Ho, T.Y., Liang, J.A., Hsiang, C.Y. 2008. Histidine residue at position 226 is critical for iodide uptake activity of human sodium/iodide symporter. J. Endocrinol. 199. 213-219;

Xiao, G., Rabson, A.B., Young, W., Qing, G., Qu,Z. 2006. Alternative pathways of NF-κB activation: A double-edged sword in health and disease. Cytokine & Growth Factor Reviews 17. 281-293;

Xing, M. 2007. BRAF mutation in papillary thyroid cancer: pathogenic role, molecular bases, and clinical implications. Endocr Rev. 742–762;

Xing, M., Alzahrani, A.S., Carson, K.A., Viola, D., Elisei, R., Bendlova, B., Yip, L. 2013. Association between BRAF V600E mutation and mortality in patients with papillary thyroid cancer. JAMA. 1493–1501;

Xu, X., Quiros, R.M., Gattuso, P., Ain, K.B., Prinz, R.A. 2003. High prevalence of BRAF gene mutation in papillary thyroid carcinomas and thyroid tumor cell lines. Cancer Res. 63. 4561–4567;

Yabin Cheng, Guohong Zhang, Gang Li. 2013. Targeting MAPK pathway in melanoma therapy.Cancer and Metastasis Reviews;

Yamashita, A.S., Geraldo, M.V., Fuziwara, C.S., Kulcsar, M.A., Friguglietti, C.U., da Costa, R.B., Baia, G.S. 2013. Notch pathway is activated by MAPK signaling and influences papillary thyroid cancer proliferation. Transl Oncol. 197–205;

Zhang, L., Zhou, F., Dijke, P. 2013. Signaling interplay between transforming growth factor-b receptor and PI3K/AKT pathways in cancer. Trends in Biochemical Sciences. 38. 612-620;

Zhou, C., Licciulli, S., Avila, L. J., Miyoung, C., Trotman, S., Jiang, P., Kossenkov, A., Showe, C. L., Liu, Q., Vachani, A., Albelda, S. M., Kissil J. L. 2013. The RAC1 splice form RAC1b promotes K-RAS-induced lung tumorigenesis. Oncogene. 32. 903-909;

Zhu, Z., Gandhi, M., Nikiforova, M.N., Fischer, A.H., Nikiforov, Y.E. 2003. Molecular profile and clinical-pathologic features of the follicular variant of papillary thyroid carcinoma. An unusually high prevalence of RAS mutations. Am. J. Clin. Pathol. 120. 71–77;

Zimmermann, M.B. 2009. Iodine deficiency. Endocr Rev. 376–408;

7. Appendixes

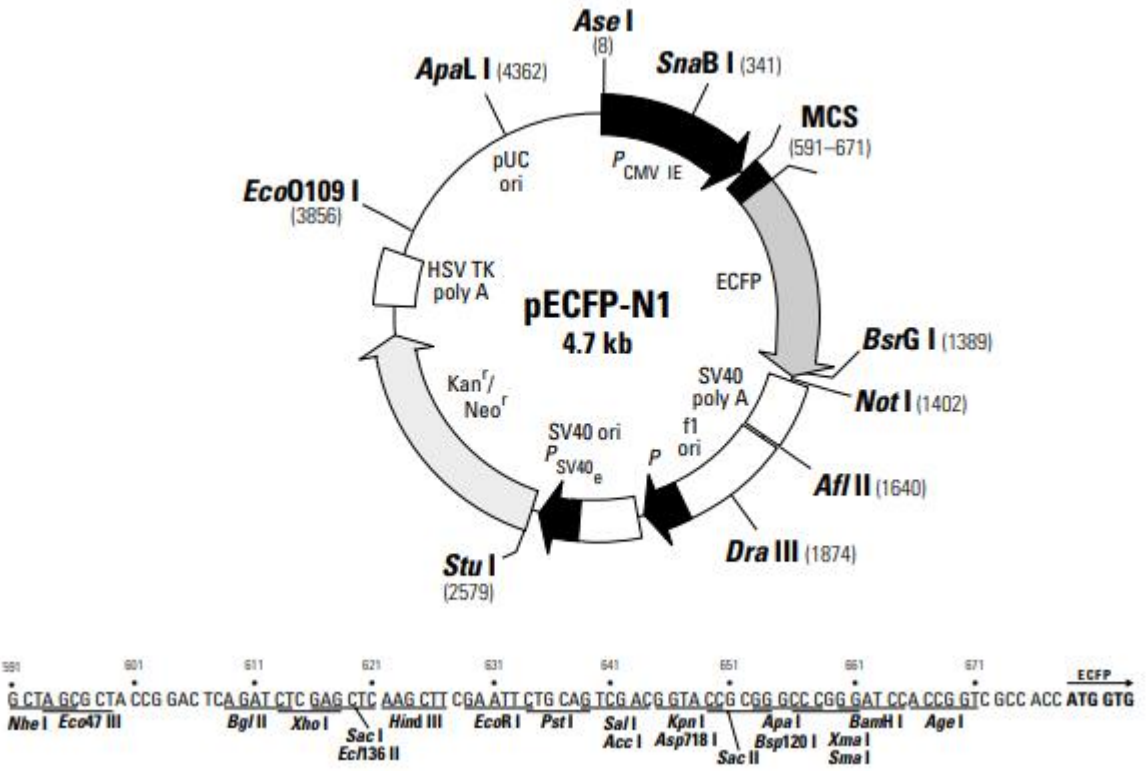

Figure 7.1 – Map and multiple cloning sites of the PeCFP-N1 vector. Human cytomegalovirus (CMV) immediate early promoter: bases 1–589; MCS: bases 591–671; Enhanced cyan fluorescent protein (ECFP) gene: bases 672-1398; SV40 early mRNA polyadenylation signal: bases 1552–1557 and 1581–1586; f1 single-strand DNA origin: bases 1649–2104; Bacterial promoter for expression of Kanr gene: –35 region: bases 2166–2171; –10 region: bases 2189–2194; SV40 origin of replication: bases 2445–2580; Kanamycin/neomycin resistance gene: bases 2629-3423; Herpes simplex virus (HSV) thymidine kinase (TK) polyadenylation signals: bases 3659–3664 and 3672–3677; pUC plasmid replication origin: bases 4008–4651. (adapted from PeCFP-N1 vector information, PT3285-5 Catalog #6900-1, BD Biosciences Clontech).

Table 7.1 – Agarose Gel Composition.

2% Agarose Gel
120 ml 1x TBE buffer 1,2g Agar 3 ml 0.05% (v/v) ethidium bromide

Table 7.2 – Lysis Buffer Composition.

Lysis Buffer
Modified Laemmli Buffer 2x 1U/µL Benzonase (*Sigma*) 2mM $MgCl_2$

Table 7.3 – SDS-PAGE Gels Composition.

SDS-PAGE Gels
Stacking gel 4%: 0,25 ml upper buffer (0,5 M tris/HCL pH 6.8) 0,2 ml 30% acrylamide 1,45 ml H_2O 20 µl 100% glycerol 20 µl 10% SDS 30 µl 10% APS 3,25 µl TEMED **Running gel 10%:** 1,15 ml lower buffer (1,5 M tris/HCL pH 8.8) 1,2 ml 30% acrylamide 2,1 ml H_2O 45 µl glycerol 45 µl 10% SDS 67,5 µl 10% APS 5 µl TEMED **Upper Buffer (0,5 M tris/HCL ph 6,8):** 15,14g Tris HCL H_2O until 250 ml **Lower Buffer (1,5 M tris/HCL pH 8.8):** 45,43g Tris HCL H_2O until 250 ml

Table 7.4 – Western Blot Solutions Composition.

Western Blot Solutions	
Sample buffer (SB) 2x: 200mM Tris-HCL 10% (w/v) SDS 325mM DDT 25% (v/v) glycerol 0.05% bromophenol blue pH 6.8 **SDS- Page buffer 10x:** <u>For 2,5 L</u> 25g SDS 76g Tris 360,3g glycine H_2O until 2,5 L **Blot buffer 25x:** <u>For 1L</u> 1,25g SDS 145g Tris 72,5g glycine H_2O until 1L **Coomassie destain:** <u>For 200 ml</u> 20 ml acetic acid 90 ml methanol H_2O until 200 ml	**Coomassie (stain):** <u>For 500 ml</u> 1,25g brilliant blue G (*Sigma*) 225 ml methanol 50 ml acetic acid **TBST:** <u>For 1L</u> 2 TBS tablets 500 µl triton x-100 H_2O until 1L **ECL solution 1:** 980 µl 100mM Tris-HCL pH 8.8 15µl 250mM Luminol 5µl 90µM cumaric acid **ECL solution 2:** 1 ml 100mM Tris pH 8.8 1 µl 7% (v/v) H_2O_2

Table 7.5 – Biotinylation Solutions Composition.

Biotinylation Solutions	
PBS-CM: <u>For 400 mL</u> 2 PBS tablets bring the volume to 400ml with ddH2O 400 µL $CaCl_2$ 1M 400 µL $MgCl_2$ 1M **TRIS-Q:** <u>For 50 mL</u> 5 mL Tris/HCl pH 7.5 1 M 1.5 mL NaCl 5 M 50 µL $CaCl_2$ 1M 50 µL $MgCl_2$ 1M 500 µL Glycine 1M 0.5 g BSA **Wash Buffer:** <u>For 50 mL</u> 5 mL Tris/HCl pH 7.5 1 M 3 mL NaCl 5 M 5 mL Tx-100 10 %	**PD Buffer:** <u>For 25 mL</u> 1.25 mL Tris/HCl pH 7.5 1 M 0.5 mL NaCl 5 M 2.5 mL Glycerol 100 % 2.5 mL NP40 10 % 250 µL SDS 10 %